Babeș-Bolyai University, Cluj-Napoca
Faculty of Geography
Doctoral School of Geography

DOCTORAL THESIS

-Summary-

Peak flows determination using a GIS-based methodology for flood risk assessment. Applications to small watersheds in the middle mountainous area surrounding the Brașov Depression.

Doctoral Supervisor
Prof. Dr. Ioan Aurel IRIMUȘ

PhD candidate
Carina STRAPAZAN

CLUJ-NAPOCA
2023

CONTENTS

Keywords: NRCS-CN method; median; asymptotic fitting; geometric mean; Brașov Depression; Mike Hydro River; HEC-HMS;SCS; GIS

1. INTRODUCTION

Over the last 20 years, Europe has experienced an increasing frequency of extreme weather phenomena such as droughts and heavy rainfall with associated floods (Hänsel et al., 2022) that caused significant economic losses as well as human casualties. The increased frequency and intensity of such phenomena triggered catastrophic consequences in many regions and the effects are still strongly felt by the populated areas located within small watersheds in Romania, some of which with a precarious state or even lack of flood protection infrastructure.

There is a crucial need for rainfall-runoff process modelling, especially in this country, where such areas are represented by a poor density of monitoring sites.

1.1. Research aim and objectives

In Romania, the rational method is generally applied for peak runoff estimation from small, ungauged watersheds, while the American NRCS-CN method is less used for hydrological practices.

The current research stems from the hypothesis according to which the NRCS-CN method could be a solid alternative for peak runoff and flood events estimation in ungauged basins located within the country. A series of steps needed to be carried out in order to achieve this goal, as follows:

- Determination of CN values by applying both the traditional procedure of using the lookup tables provided in the literature and the rainfall-runoff methods based on locally measured data. Following the obtained results, a comparative analysis on the applied methods will be carried out based on the runoff estimates from the study watersheds.
- Flood hydrographs simulation based on the abovementioned CN values, using three types of hydrological models: lumped, semi-distributed and distributed parameter models.

Another hypothesis of interest refers to the relationship that generally emerges between CN and rainfall depth, which can only be defined based on measured data along with the fact that the use of lookp tables without site-specific validation may lead to inaccurate results. The study watersheds are located within the mountain region surrounding the Brașov

Depression. The selection was based on the fact that the area is represented by a limited number of monitoing stations, being prone to flood hazards, endangering the local activities and population. Over the past 20 years such significant rainfall-runoff events have been recorded in 2010, 2016 and 2018, with the largest historical records in the latter 2 years.

Even though each of the study watersheds is equipped with a gauging station, their ungauged and flash flood prone tributaries pose serious threats to the local activities. The forestry institutions conduct important activities within the area that often end up being interrupted, given that the forest roads along the tributaries are frequently affected by flash flood events.

In fact, Covasna is one of the most affected counties in Romania when it comes to floods. Therefore, a secondary goal of this paper is the peak flows estimation in the upstream catchments of Covasna and Ozunca rivers, using the abovementioned method and the semi-distributed model.

2. THE CURRENT STATE OF NATIONAL AND INTERNATIONAL RESEARCH

The **NRCS-CN** method**,** formerly known as the Soil Conservation Service-Curve Number (SCS-CN), developed in 1954 and initially published by the Soil Conservation Service in Section 4 of the National Engineering Handbook (NEH-4), is based on the equation for computing total runoff from rainfall (NRCS,2004):

$$Q = \frac{(P - Ia)^2}{P - Ia + S} \qquad \text{for } P > Ia,$$

$$Q = 0 \qquad \text{for } P \leq Ia,$$

$$Ia = \lambda S \tag{1}$$

$$S = 25.4\left(\frac{1000}{CN} - 10\right) \quad \text{or} \quad CN = \frac{25400}{254 + S} \tag{2}$$

Unde:

P is the rainfall amount (mm);

Ia stands for the initial losses (mm);

S is the potential maximum retention (mm).

The CN index (dimensionless), usually determined from the standard NRCS tables originally published in NEH-4, which are now given in the NEH-630 documentation (NRCS,2004), encompasses the runoff-producing characteristics of drainage basins such as soil type, land use/land cover and hydrologic conditions (Mishra & Singh, 2003; D'Asaro et al., 2014; Gyori et al., 2016).

The NRCS tables have been adapted to the territorial features of Romania by Chendeș (2007) and later also presented in other works (Drobot, 2007; Chendeș, 2011).

The method was initially developed based on field research conducted in small agricultural watersheds across the U.S. (Ponce & Hawkins, 1996), over the years, its usage being extended to rural, forested or urban ones with the original approach assuming the constant value of 0.2 for the λ coefficient in practical applications (Mishra & Singh, 2003). Subsequent studies have demonstrated the shortcomings in applying this constant, superior results being achieved for $\lambda = 0.05$ (ex. Hawkins et. al., 2009; D'Asaro et al. 2014), thus recommending further redefinition of the NRCS tables.

There are several studies that applied the method to various watersheds in Romania such as the ones conducted by Man and Alexe (2006), Crăciun et al. (2009), Crăciun (2011), Domnița (2012), Gyori (2013), Costache (2014), Gyori et al. (2016), Zaharia et al. (2017), Kaffai-Voda (2022) etc.

Given that the development of the method has been mostly based on information collected from agricultural basins (Hawkins et. al., 2009) and that the NRCS tables provide a wide range of CN values representative of various land uses and covers including forested areas, which for the tropical and temperate regions have not yet been validated (Im et al., 2020), at a local level, their use involves uncertainties, with calibrations of locally measured data being mandatory (Hawkins et. al., 2009, Strapazan et al., 2023a). The CN values thus obtained (CN II) following the classical procedure correspond to AMC II (normal antecedent moisture conditions), requiring conversion to AMC I (dry conditions) or III (wet conditions) based on the 5-day rainfall depth prior to the onset of the runoff event, based on the threshold values provided in the 1964 edition (SCS, 1964). These criteria have been removed from the later NRCS versions, and the term "Antecedent Runoff Conditions" (ARC) came into use in 1993, replacing the "AMC" one, thus accounting for the numerous additional factors defining the rainfall-runoff relationship (Hawkins et al., 2019).

However, related studies carried out in Romania based on the CN index method relied on the NRCS-CN tables and the traditional AMC determination procedure, given the many

ungauged or poorly gauged local basins, and the relatively short data records available (Strapazan et al., 2023a).

Various studies in the literature have developed or applied different methods to determine CN values based on measured *P*-*Q* (rainfall-runoff) data: asymptotic fitting (e.g. Hawkins, 1993; D'Asaro et al., 2014; Calero Mosquera et al., 2021), median (e.g. Ajmal et. al., 2016; Ibrahim et al., 2022), geometric mean and arithmetic mean methods (e.g. Tedela et al., 2012; Ibrahim et al., 2022). Many studies revealed the presence of a general tendency of CN values stabilization towards higher rainfall amounts, the index being rather a variable that takes different values from event to event (Hjelmfelt, 1991; Ponce & Hawkins, 1996; Strapazan et al., 2023a). The NEH-4 method is an approach that excludes this generally known tendency of CNs to decrease with increasing rainfall, which is why it can lead to systematic errors (Hawkins et. al., 2009).

2.2. Types of hydrological models and the main steps of the modelling process

One of the major hydrological concerns is the rainfall-runoff relationship of which analysis has evolved over time, from simple expressions and techniques to the complex mathematical models commonly used nowadays.

Chow et al. (1988) classify models into physical (scale and analog) and abstract (mathematical) models including the deterministic ones. The latter are further divided into: distributed-parameter models (white-box) accounting for the spatial variability of the parameters (Abbott & Refsgaard, 1996), empirical models (black-box) based entirely on the system's inputs and outputs (Beven, 2012), and conceptual models (gray-box) with lumped parameters (Gyori, 2013).

There is also an intermediate variant between distributed and lumped-parameter models, namely the semi-distributed ones, which divide the watershed based on the common properties of interest. The parameters' distribution is considered either according to hydrological response units or subwatersheds areas boundaries (Gyori, 2013). According to spatial variability of the modeled system's characteristics, the models can thus be divided into lumped, semi-distributed, and distributed-parameter models (Crăciun, 2011). An example of the spatial structure in hydrological models can be seen in Figure 1.

Since 1960, the emergence of computers has led to the development of computerized hydrological models, which have become an essential tool, especially for problem-solving in in hydrology (such as the ungauged basins analysis), so that the process automation facilitated

the entire procedure (e.g., Stanford model, KINEROS2, SHE, MIKE HYDRO River, HEC-HMS, etc.).

MIKE HYDRO River is a powerful tool for 1D hydraulic and hydrodynamic modeling, which includes 4 types of hydrological, lumped-parameter models associated with the embedded rainfall-runoff module (DHI, 2017). The model has been used in several studies, conducted both internationally and in Romania (e.g., Ivănescu et al., 2014; Talchabhadel & Shakya, 2015; Bălan et al., 2016; Kocsis et al., 2020).

HEC-HMS is a software package developed to simulate runoff from a watershed taken as a system with interconnected hydrological and hydraulic components (USACE, 1998). It has been used for runoff estimation from small-sized catchment areas by many authors such as Gyori and Haidu (2011), Gyori et al. (2013), Khaddor and Alaoui (2014), Haidu and Ivan (2016), etc.

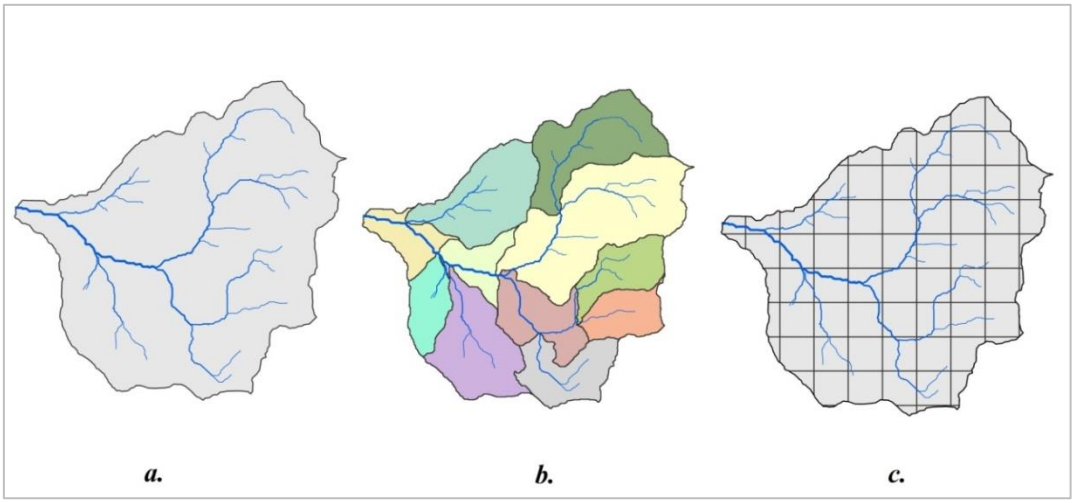

Figura 1. The spatial structure of hydrological models: a.lumped model; b. semi-distributed model by subwatershed; c. distributed model

The development of GIS products over recent decades has led to the emergence of a variety of modules and extensions that aid in the analysis and performance of hydrological computations (e.g., AGWA, Hec-GeoHMS, ArcHydro, ArcSWAT).

The present research will use two modeling softwares, namely HEC-HMS and MIKE HYDRO River, along with the Cluj distributed-parameter model. The results will be compared in order to identify an optimal procedure for NRCS-CN method application in the study area.

3. GEOGRAPHICAL LOCATION OF THE STUDY WATERSHEDS

The doctoral thesis focuses on the analysis of 4 gauged catchment areas located in the central part of Romania (Figure 2). The hydrometric stations belong to the Romanian Waters National Administration, Brașov and Covasna Water Management Systems.

All the studied sites belong to the upper Olt River basin and fall into the category of small-sized basins, which, according to the Institute of Meteorology and Hydrology (1971), have catchment areas smaller than 100 km^2 and require increased attention of their hydrologic behavior.

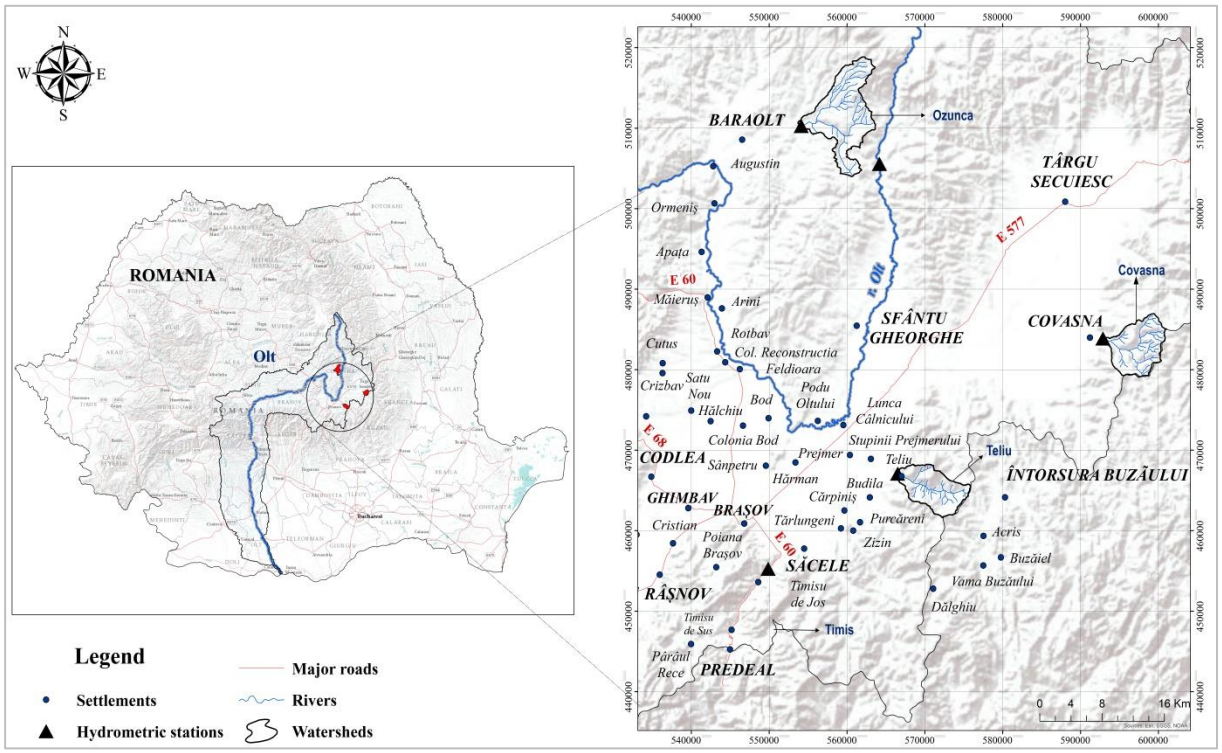

Figure 2. Geographical location of the study watersheds (modified after Strapazan et al., 2023a)

The study areas are located within the mountain region surrounding the Brașov Depression (Figure 3). The present research was conducted on the headwater, mountainous areas of the watersheds, belonging to the middle mountainous region of Romania, with the gauging stations considered here as outlet points.

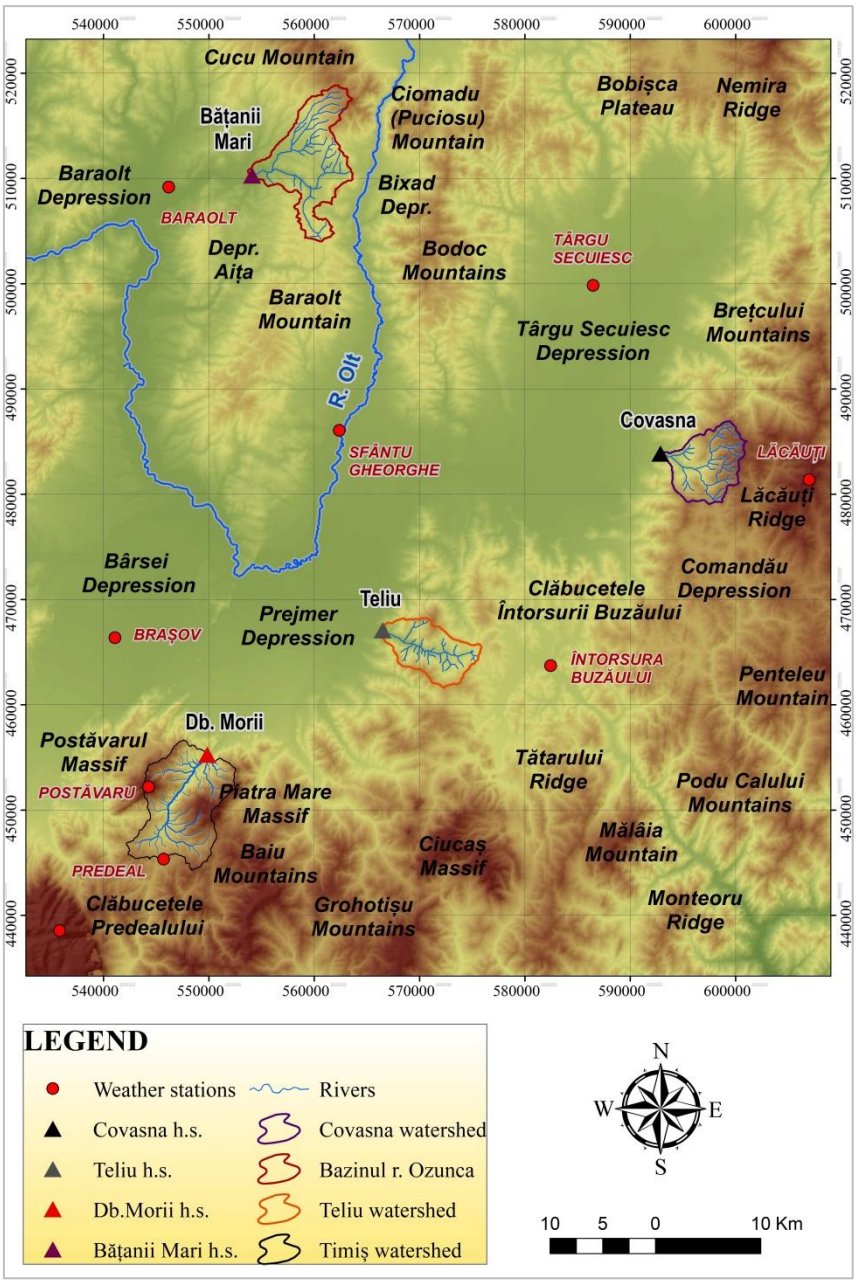

Figure 3. The main relief units and monitoring sections

4. CREATING THE DATABASE FOR SURFACE RUNOFF MODELLING

4.1. The numerical database

The data collected for this research belong principally to a maximum time series length between 1991 and 2020 and was provided by the ”Olt” Water Basin Administration - Brașov and Covasna Water Management Systems, as well as the National Institute of

Hydrology and Water Management (I.N.H.G.A.) and the National Meteorological Administration (N.M.A.).

- *meteorological data* – historical daily records, weather warnings, and recorded data during floods. Data related to rainfall intensity and duration from the meteorological stations (m.s.) Lăcăuți and Întorsura Buzăului were also used, as well as records from m.s. Predeal and the hydrometric station (h.s.) Micfalău. Radar rainfall estimates (hourly accumulations) provided by the N.M.A. were also used. In order to obtain the gauge-corrected radar-based estimates, information available from the following m.s. was used: Vf. Omu, Brașov-Ghimbav, Miercurea Ciuc, Târgu Secuiesc, and Sfântu Gheorghe. The information used from the m.s. was extracted from the Meteomanz (Meteomanz, 2017) and RP5 (RP5, 2017) databases: http://meteomanz.com/, https://rp5.ru/.
- *hydrological data*- historical records gathered from the 4 h.s. located within the watersheds (Table 1).

Table 1. Data description

Watershed	Hydrometric station	The time range of the observational data used	Data series	No. of events
Teliu	Teliu	1991-2020	discharge data, daily rainfall, flood events	57
Timiș	Db. Morii	1993-2020	discharge data, daily rainfall, flood events	64
Covasna	Covasna	2004-2018	discharge data, daily rainfall, flood events	34
Ozunca	Bățanii Mari	2004-2018	discharge data, daily rainfall, flood events	32

4.2. The cartographic database

- A *topographic map (scale 1:25.000)* was used in order to generate a digital elevation model (DEM) through interpolation of digitized contours. For a comparative analysis and automatic identification of watershed areas, the European Union Digital Elevation Model *(EU-DEM) v1.1* was also used. This model was downloaded from the following website: https://land.copernicus.eu/ and made available for general use through the Copernicus programme (Mouratidis & Ampatzidis, 2019; Strapazan et al., 2019; Strapazan et al., 2021; Strapazan et al., 2023b).

- *Soil map (scale: 1:200,000)* for Romania created by the National Research and Development Institute for Soil Science, Agrochemistry and Environment (ICPA-Romania).
- *Land use/land cover maps* taken from the *Corine Land Cover (CLC)* database, made available for general use through the Copernicus programme (EEA, 2017, 2018, 2020). CLC data from 2006, 2012, and 2018 was used in order to conduct a comparative analysis, considering data revisions over time along with the possibility of changes in the land use pattern, which can lead to different CN values (Strapazan et al., 2023a).
- The spatial dataset for the *1:200,000 scale geological map*, created by the Geological Institute of Romania and made available on the following website: https://geoportal.igr.ro/viewgeol200k and it was accessed for informational purposes using the visualization services.

4.2.1. Automatic delineation of watershed boundaries and stream networks using the ArcHydro module

The starting point in this research was to analyze the accuracy of input data from various sources used as a basis for surface runoff determination and flood events modeling. Thus, the accuracy of EU-DEM in deriving primary terrain attributes related to watershed areas was evaluated, and the obtained elevations were compared with those generated from the DEM derived from contour lines (with a resolution of 10 m). Considering the small-sized watershed areas (< 100 km^2), the use of EU-DEM was a reasonable choice due to its higher resolution compared to available ASTER and SRTM data.

In order to obtain the stream network and the catchment delineation, the available ArcHydro model functions were used. The process involves a considerable number of steps, such as filling the artifact sinks resulting from DEM creation, computing the flow direction, flow accumulation, and so on (Kraemer & Panda, 2009). Accordingly, a model was implemented in ArcGIS, v.10, using Model Builder in order to automate the tasks and the entire process, thus reducing the execution time (Strapazan & Petruț, 2017; Strapazan et al., 2019; Strapazan et al., 2021). The model incorporates all ArcHydro functions used for watershed and stream network delineation (Figure 4).

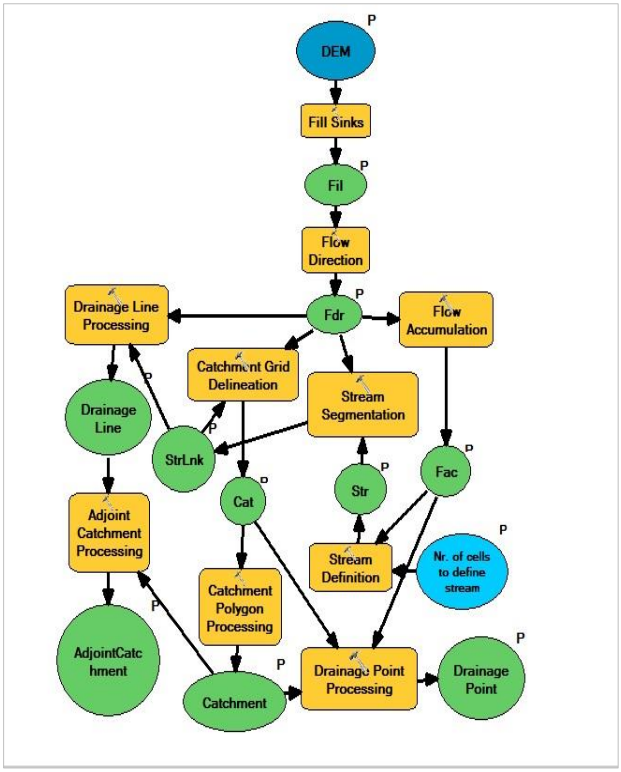

Figure 4. The model for the ArcHydro process

(Strapazan & Petruț, 2017)

4.2.2. The derived GIS database and watersheds' defining features.

The natural factors that play a determining and conditional role for the surface runoff occurence include both climatic (determining role) and geological, terrain, soil, and vegetation-characteristics related factors, the latter being the conditional factors affecting runoff generation (Mustățea, 2005). The obtained catchment areas based on the ArcHydro techniques, range from 36 to 75 km^2 (corresponding to the monitoring sections), with mean elevation values that vary between 746 m and 1108 m, maximum elevations of up to 1842 m, and minimum values starting from 510 m. The average slopes range between 16.66% and 36.43% (Table 2).

Table 2. Morphometric characteristics of the study watersheds

Bazine hidrografice	**Suprafața (km^2)**	**Altitudinea medie (m)**	**Panta medie (%)**	**Altitudinea maximă (m)**	**Altitudinea minimă (m)**
Teliu	36	801	24.92	1212	540
Timiș	75	1108	36.43	1842	682
Covasna	39	1037	29.39	1467	600
Ozunca	66	746	16.66	1356	510

Elevation, aspect and geological features

The mean elevation found for the **Teliu** River basin is 801 m, with a highest value of 1212 m (towards Pilișca Peak) and a lowest elevation of 540 m, derived from DEM (based on contour lines) processing, with very small differences compared to those associated with the EU-DEM (max. = 1212.1 m, mean = 801.4 m and min.= 540.3 m). The hydraulic length computed through the ArcHydro functions is 11.35 km. The shady and cool north-facing slopes are the most dominant (19.84%) within the area. The west and northwest-facing slopes cover ≈ 27% of the basin's area. The watershed lithology is mainly represented by sandstones, marls, and conglomerates.

The analysis of the contour-derived DEM indicates a value of 1842 m for the highest elevation in the **Timiș** watershed, as opposed to the one of 1828 m derived from the EU-DEM, and a minimum value of 682 m corresponding to the northernmost portion of the catchment where the hydrometric station is located (similar to the value obtained from EU-DEM processing = 681.6 m). The computed hydraulic length is 17 km. Given the valleys orientation, shady slopes predominate, covering ≈ 17% of the total area. Mountain slopes receiving higher precipitation amounts account for 27.54% of the total area. The underlying bedrock consists of conglomerates, sandstones, limestones, and marls.

The mean elevation found for the **Covasna** River basin is 1037 m, with a highest value of 1467 m, and a lowest elevation of 600 m (corresponding to the depression area), resulting from the analysis of the DEM (derived from contour lines). The EU-DEM data indicates similar values (mean = 1035 m; max. = 1469 m; min. = 600 m), thus the area falls within an elevation range of 867 m. Considering the general valleys orientation, west-facing slopes predominate (19%). The west and northwest-facing slopes cover ≈ 36% of the catchment area. The entire catchment area is located within the external Carpathian Flysch zone, with flysch sandstones (Tarcău Sandstone facies) and flysch sandstones with shist intercalations occupying most of the watershed from its upper to middle sectors.

The computed hydraulic length corresponding to the **Ozunca** watershed is 15.5 km, and the analysis of the contour-derived DEM indicates a maximum elevation value of 1356 m (towards Pilișca Mare Peak), a mean value of 746 m, with the lowest elevation value of 510 m corresponding to the westernmost portion of the watershed, close to the hydrometric station location. Thus, the watershed falls within an elevation range of 846 m, with small differences compared to the values obtained from EU-DEM processing (mean = 745 m and min. = 511 m), except for the highest value, which in this case is 1370 m. The west-facing slopes

receiving higher rainfall amounts are the most dominant covering up to 18.4% of the catchment area (together with the northwest-facing slopes accounting for 31.2%, slightly lower compared to Covasna watershed). The largest portion of the watershed is occupied by Neocomian deposits (Sinaia beds), and around the volcanic cones, the bedrock consists mainly of Neogene andesites with amphiboles and biotite, amphiboles and pyroxenes, and with Neogene pyroxene andesites.

Terrain declivity

The **Teliu** watershed is mostly characterized by slopes ranging between 5-15^0 (≈ 49.5%). The dominant relief feature of the **Timiș** River basin is the presence of steep slopes with high relief energy and torrential activity, with slopes ranging from 25-35^0 that account for ≈ 28% of the total area. Similarly, slopes ranging between 5-15^0 cover ≈ 27% of the area, especially in the upper sector of the basin where the Timișul de Sus Depression is located.

Regarding the **Covasna** basin, the largest portion of its area (43%) is characterized by slopes ranging from 5-15^0, with an average slope of 29.4%. The **Ozunca** watershed, is mostly characterized by slopes ranging from 5-15^0 (49%), followed by gentle slopes of 2-5^0 (29%).

Land use/land cover, vegetation and soils

The **Teliu** River basin is characterized by a high forest coverage of 70.5%, with broadleaf forests being representative (63.7%). Pastures occupy significant areas within the watershed (20.7%), while transitional woodland-shrub and agricultural lands cover much smaller areas within the upper sector of the basin. The analysis of CLC 2018 data, indicated the highest percentage of forest cover (92.4%) for the **Timiș** watershed. Broadleaf and mixed forests have relatively similar proportions within the area (23-25%). The forest cover percentage corresponding to the Covasna watershed is 81.5%, with coniferous forests being the dominant land cover (≈ 70% of the total area). Transitional woodland-shrubs (usually deforested) account for 13.3% of the land area within the watershed. Forests cover less than 56% of the total catchment area of **Ozunca** (compared to the other ones under study) with broadleaf species predominating (52.3%). A quite large portion of the area is occupied by natural grasslands (21.3%).

Dystric Cambisols cover the largest areas within the study watersheds: 66.2% in the Teliu River basin, 78% in the Timiș watershed and 73% of the Covasna catchment area. Eutric Cambisols predominate covering almost 48% of the total drainage area of the Ozunca River, and Luvisols are also widespread within the watershed (40%).

5. RESEARCH METHODOLOGY EMPLOYED FOR MAXIMUM RUNOFF AND FLOOD EVENTS SIMULATION BASED ON THE NRCS-CN METHOD

5.1. CN determination methods

Five methods will be used to determine the CN values associated with the growing season. These are: the tabular method (TAB), namely the classical procedure of deriving the values from the handbook tables; the asymptotic fitting of both ordered (AF_O) and natural, unordered data (AF_N); median (MD); geometric mean (GM) and arithmetic mean (AM) methods. In other words, this research addresses the applicability of the traditional procedure for determining CN values in comparison to the use of rainfall and discharge records in order to obtain these values (Strapazan et al., 2023a). All the calculations were performed both for the original NRCS initial abstractions coefficient $\lambda = 0.2$ and for $\lambda = 0.05$, which is often suggested in the literature.

5.1.1. Database processing

For the analysis, all the available 187 *P-Q* (rainfall-runoff) events belonging to the maximum time series length between 1991 and 2020 were used and rainfall spatialization was performed within a GIS environment based on the Thiessen polygon method (Strapazan et al., 2023a). The daily records correspond to the period from April to October when surface runoff is predominantly rainfall-driven. Both the ordered and unordered *P-Q* datasets were used for the application of the asymptotic fitting method. All the data used for the central tendency methods (MD, GM, AM) application were subjected to several analysis procedures, meaning that partial data pairs were removed, and with the aim of avoiding possible systematic errors associated with low precipitation amounts, only those events where $P > 25.4$ mm [1 inch] (Hawkins et al. 2009) and $P/S > 0.46$ (Hawkins et al., 1985) were selected. The largest 22 events (recorded at Teliu and Dâmbu Morii hydrometric stations) and 17 events (recorded at Covasna and Bățanii Mari hydrometric stations) from the entire data series were selected for the central tendency methods application (Strapazan et al., 2023a).

The constant slope model included in the Cavis software developed by Corbuș (2010) was used in order to obtain the direct surface runoff (Figure 5):

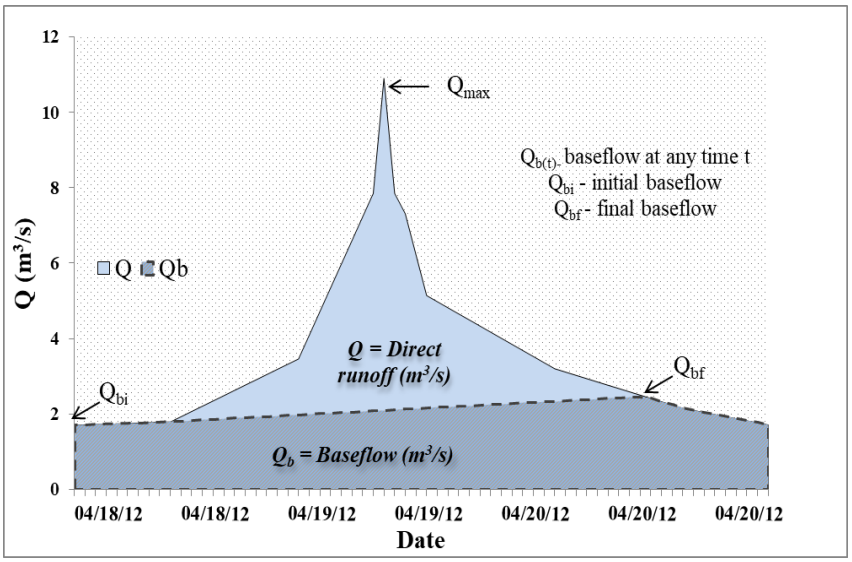

Figure 5. Graphical representation of the baseflow separation method. An example of the separation results for the representative runoff event in April 2012 recorded at the Teliu gauge station (after Strapazan et al., 2023a)

5.1.2. NRCS-CN tabular method (TAB)

The CN parameter is a function of land use/land cover and hydrologic soil groups (HSG). Accordingly, soils are classified into 4 hydrologic groups (A, B, C, and D) based on the rate of water infiltration (USDA-NRCS, 1986).

Given that the present research addresses the issue from a lumped perspective, the area-weighted CN calculation for each watershed was necessary according to the following equation (USACE, 2000):

$$CN_w = \frac{\sum_{i=1}^{n} CN_i A_i}{\sum A_i} \quad (3)$$

Where: CN_w – area-weighted CN; CN_i –CN value associated with each land use-soil combination; A_i – the area for each land use-soil combination; n–no. of land use-soil combinations.

The calculation of weighted average CNs was based on CLC data from 2006, 2012, and 2018, with the purpose of conducting a preliminary analysis of the differences in CN values that may result from different databases. The resulting differences were extremely small, ranging from 0.2 (for Teliu and Ozunca watersheds) to 0.9 (for Timiș River basin). For this reason, and also considering CLC datasets updates, in 2018 for the first time consistent and higher-quality data from the European Copernicus Programme's Sentinel-2 satellites

being used (Cole et al., 2022), the tabulated CNs established and used in this study are based on the land use patterns derived from the CLC 2018 database (Strapazan et al., 2023a). In order to reduce the time required for deriving these values, the process has been performed through Model Builder based on Hec-GeoHMS functions (Figure 6).

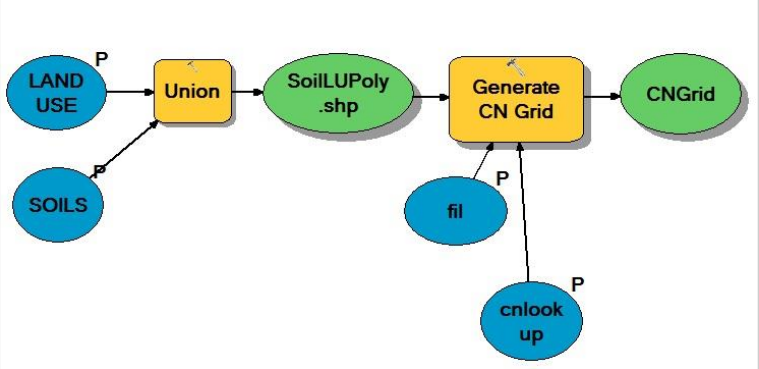

Figure 6. The model for obtaining the CN values based on HEC-GeoHMS functions (Strapazan & Petruț, 2017)

In the present research, for the classical or standard application of the NRCS-CN method, which involves converting CN_{II} values, the effects of AMC were considered through a preliminary analysis for which the *P*-*Q* events were classified based on both the 5 and 10-day precipitation totals prior to the onset of the runoff events. This analysis was conducted considering the coefficient of determination (R^2) in order to determine whether the AMC classes justify the increases in surface runoff in relation to precipitation (Strapazan et al., 2023a). The results showed that the variation in surface runoff seems to be explained to a greater extent by the rainfall amount when 10 days are considered (Figure 7). The conversiom of CN_{II} values to dry or wet antecedent conditions was made possible by using the equations recommended by Mishra et al. (2008), which have also been applied in other studies such as Ajmal et al. (2016):

$$CN_I = \frac{CN_{II}}{2.2754 - 0.012754CN_{II}} \quad (4)$$

$$CN_{III} = \frac{CN_{II}}{0.430 - 0.0057CN_{II}} \quad (5)$$

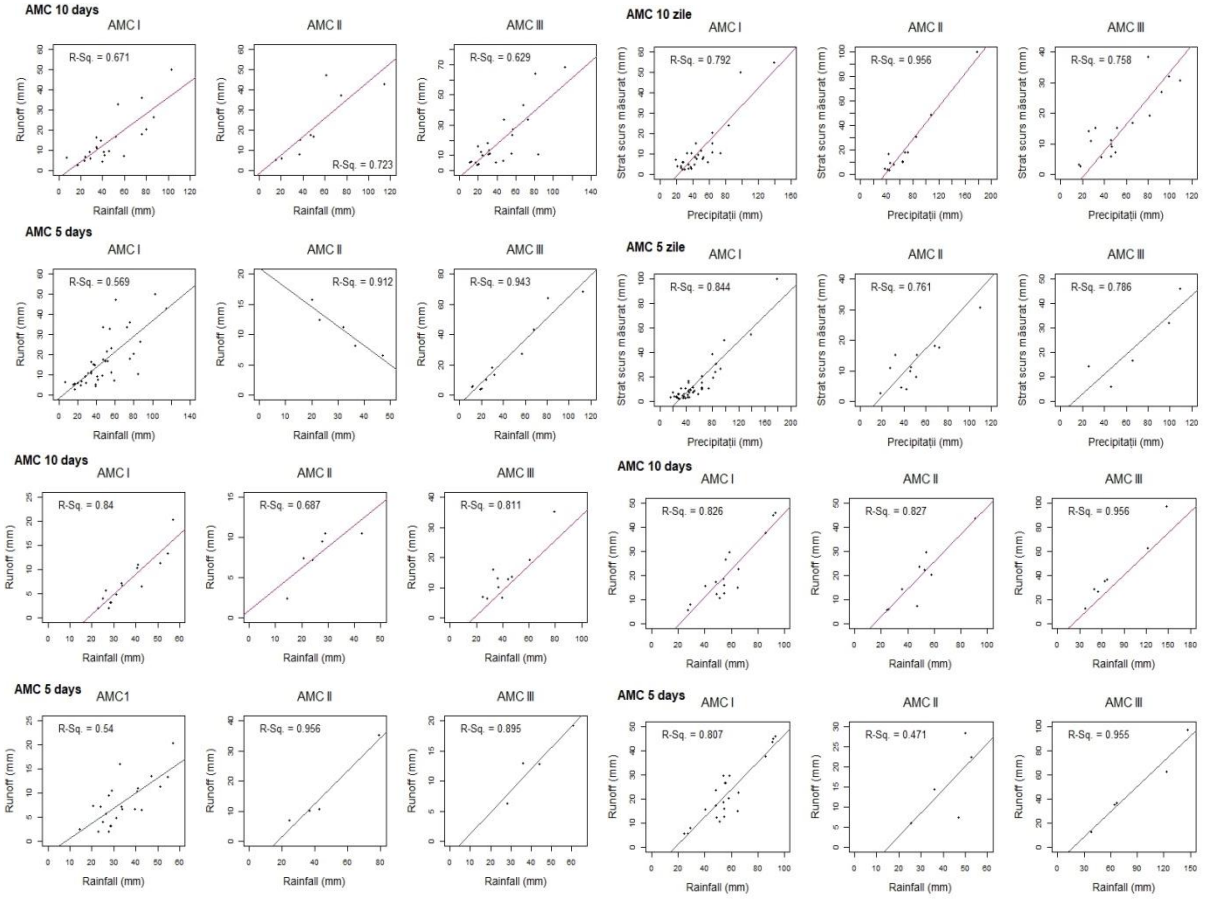

Figure 7. Rainfall-runoff relationship for the AMC-5 and AMC-10 for: a) Teliu, b) Timiș, c) Ozunca și d) b.h. Covasna (modified after Strapazan et al., 2023a)

5.1.3. Rainfall-runoff data-based methods

When data records from the hydrometric and meteorological stations are available, the S value cand be determined for $\lambda = 0.2$ by solving Equation (1) [Ch.2] and a series of algebraic calculations (Hawkins, 1993) and the CN vlues can be obtained directly by substitution:

$$S_{0.2} = 5\left[P + 2Q - (4Q^2 + 5PQ)^{0.5}\right] \tag{6}$$

$$CN_{0.2} = \frac{25400}{254+5(P+2Q-\sqrt{4Q^2+5PQ})} \tag{7}$$

For the conversion of CN and S values for $\lambda = 0.05$ directly from the $\lambda = 0.2$ results, Woodward et al. (2003) suggest the following expressions:

$$CN_{0.05} = \frac{100}{1.879(100/CN_{0.2} - 1)^{1.15}+1} \tag{8}$$

$$S_{0.05} = 0.8187 S_{0.2}^{1.15} \quad (9)$$

Considering λ = 0.05, based on a sequence of algebraic calculations, $CN_{0.05}$ can be directly determined (Ajmal et al., 2016):

$$CN_{0.05} = \frac{100}{1+0.0393701\left[2P+19Q-\left(361Q^2+80PQ\right)^{0.5}\right]} \quad (10)$$

- *Median CN method (MD)*

The values of CN and S were derived by solving Equations (1) and (6). Subsequently the CN index was adjusted for λ = 0.05 using Equation (8). Finally, the median of the CN values was extracted for further analysis (Strapazan et al., 2023a).

- *Geometric Mean CN method (GM)*

The method was applied by taking the logarithm of S, previously determined through Equation (6), followed by the arithmetic mean calculation of *log(S)*, and subsequently, the geometric mean S, 10^{logS}. Finally, the CN values were estimated as follows (Tedela et al., 2012, Ajmal et al., 2016):

$$CN_{GM} = \frac{25400}{(254 + 10^{logS})} \quad (11)$$

- *Arithmetic Mean CN method (AM)*

As it is also a central tendency method, it was used by first applying Equations (2) and (6) to calculate the CN and S values, and subsequently by extracting the representative CN value from the dataset. (Strapazan et al., 2023a).

- *Metoda asymptotic fitting (AF-aproximare asimptotică)*

The method considers the CN index as an asymptotic limit as P approaches ∞. The relationship between CN and P is graphically represented, and the asymptotic CN value associated with significant rainfall amounts is taken as the final representative value at the watershed level (Cao et al., 2011). In order to apply this method, all the available *P-Q* events from the gauging stations were used, but they were separately sorted in descending order. The resulting CN values from Equations (2) and (6) correspond to each *P-Q* pair of independently

ordered data (referred to as the AF_O method). Additionally, the method was also employed on the natural, unordered dataset (referred to as the AF_N method).

By plotting the the CN against P, Hawkins (1993) identified three types of situations: complacent, standard and violent. The complacent situation refers to the fact that the CN index does not approach an asymptotic value, and an alternative linear function may be more appropriate. The standard situation involves the tendency for CN values to decrease and then approach constant values with increasing rainfall depth. Hawkins (1993) described this situation as follows:

$$CN(P)= CN_{\infty}+(100-CN_{\infty}) \exp(-k_1 P) \quad (12)$$

Where:

CN_{∞} – constant as P -> ∞;

k_1 – fitting constant.

The violent watershed response is characterized by a sharp increase in CN values followed by a tendency to approach constant values with increasing rainfall depth (Hawkins, 1993):

$$CN(P)= CN_{\infty}[1- \exp(-k_2 P)] \quad (13)$$

Unde: k_2 – fitting constant.

5.1.4. Statistical analysis for the performance evaluation of the methods. The R software system

The performance evaluation of the CN-based methods was conducted using the R software (v. 4.2.1), which is freely available and licensed under the GNU-General Public License (R Core Team, 2022). The optimization of the *CN*∞ and *k* values for the AF method application was performed by fitting Equation (12) with the nlsLM function available in the minpack.lm package, based on the Levenberg-Marquardt algorithm (Elzhov et al., 2016). The lines of code were executed in RStudio (RStudio Team, 2022).

The performance of the CN-based methods used for estimating the runoff depth was assessed by comparing it with the measured data, using several goodness-of-fit indicators such as percent bias (*PBIAS*), R^2, root mean square error (*RMSE*), Nash-Sutcliffe model efficiency coefficient (*NSE*), and the index of agreement (*d*). The evaluation criteria in this case were those proposed by Moriasi et al. (2007), Ritter and Munoz-Carpena (2013), Diaz-

Ramirez et al. (2011) and the calculations were performed using the hydroGOF (hydrological goodness of fit) package (Zambrano-Bigiarini, 2020).

5.2. GIS methodology for rainfall spatial representation based on radar estimates

For the spatial representation of rainfall and its integration, into both the lumped-parameter model (MIKE) and the distributed GIS one, the Bias Adjustment Method was used in order to remove the average difference between the radar estimates and recorded precipitation (Steiner et al., 1999; Zhang & Srinivasan, 2010).:

$$R_{adj} = B \cdot R$$

$$B = \frac{\sum_{i=1}^{n} Z(x_i)/n}{\sum_{i=1}^{n} R(x_i)/n} \quad (14)$$

Where:

R_{adj} [mm/h] – the bias adjusted radar data;

R [mm/h] – the radar-pixel values;

B – the bias adjustment factor;

$Z(x_i)$ – the measured values at a location x_i, i = 1.2,…n;

$R(x_i)$ – radar estimated precipitation at a location x_i, i = 1.2,…n.

The radar-based rainfall information used for the study area were provided by the Bobohalma weather radar located in Mureș County.

5.3. The lumped-parameter model. MIKE HYDRO River-UHM for flood events modelling

For this study case, the MIKE Zero 2021 - MIKE HYDRO River software with a student license, provided with the support of DHI Romania, was used. Three loss estimation methods from the RR-UHM module were successively applied in the first instance, namely the NRCS-CN method (referred to by its former designation of *SCS* within the modeling system), the *SCS generalised* method, and the *Proportional loss* one, for model calibration and validation and Teliu River basin was selected as the study case. The second stage of this study was aimed at a more extensive analysis related to the previous research conducted to determine the optimal CN values for the entire study area, through both the classical approach of using the NRCS tables, and the one involving the rainfall-runoff relationship determined from measurements. The aim of the study was to validate the applicability of the CN

parameter when used for estimating flood hydrographs. These applications were carried out on all the study basins and specifically focused on the SCS embedded method. The workflow can be observed in Figure 8.

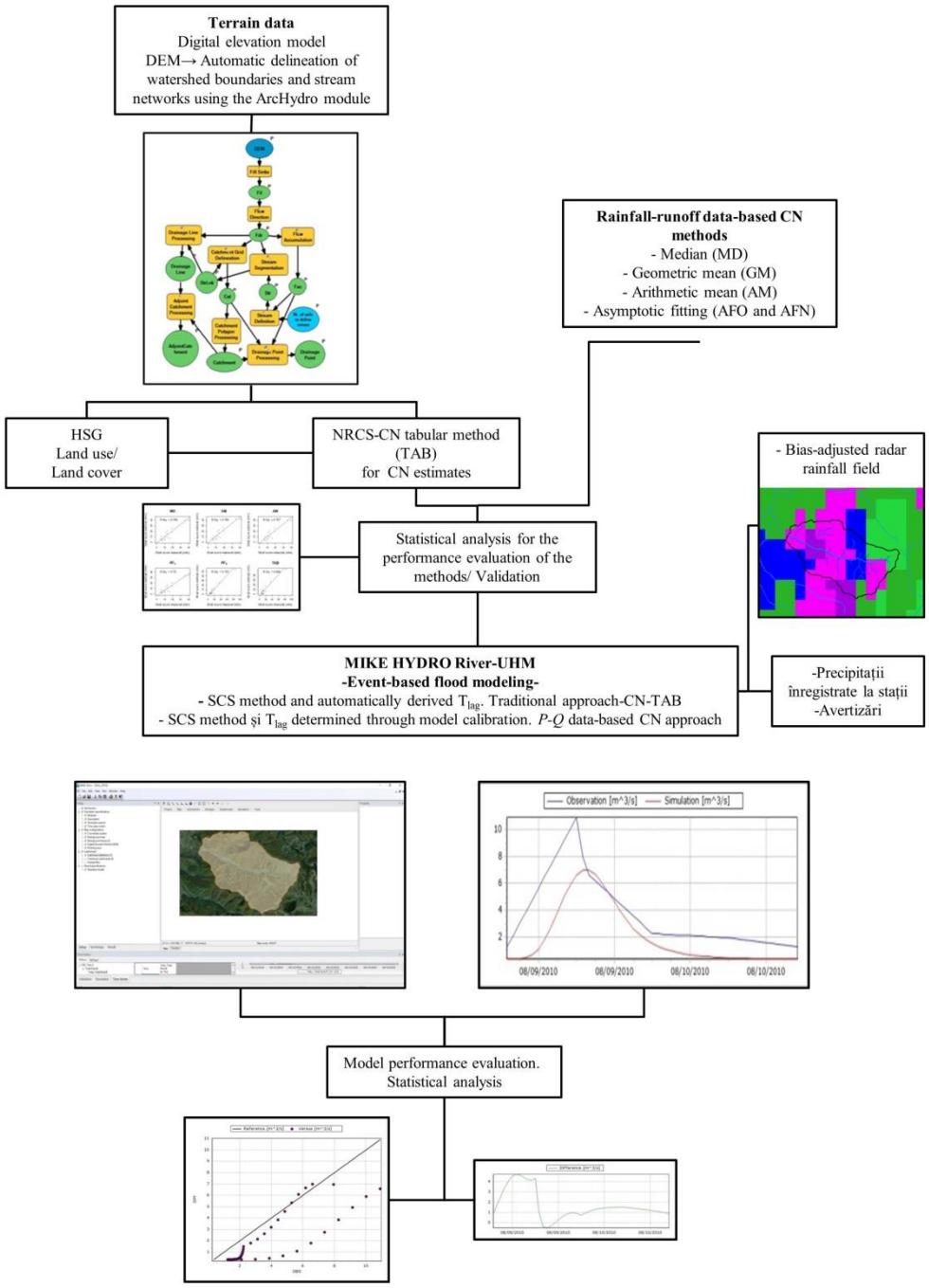

Figure 8. Overview of the workflow used in this study for flood events simulation with MIKE HYDRO River-UHM

5.4. The semi-distributed model. HEC-HMS for flood events modelling

Another aim of this research paper was to evaluate the applicability of a semi-distributed model for flood events simulation with the NRCS-CN method. For this purpose, the HEC-HMS software package was used, and its application was limited to the catchment areas of Covasna and Ozunca rivers due to the presence of more significant tributaries, contributing substantially to the total water discharge, which generally have a continuous flow of water throughout the year, unlike the other study watersheds which are characterized by the presence of intermittent tributaries with short stream lengths. Hence, the output from the ArcHydro module associated with the physical representation of the basins, was converted into an HEC-HMS project through the Hec-GeoHMS tools used to obtain the required parameters for running the model and simulate the flood hydrographs. Another aim was to conduct a comparative analysis of two different transform methods, namely the SCS method and the Snyder hydrograph one, for which Covasna River basin was selected as the study case (Strapazan & Petruț, 2017).

5.5. The distributed-parameter model. Flood events modelling by using the Cluj Model

The Cluj model, developed by the research team from the Faculty of Geography, is a GIS algorithm-based one integrating both the NRCS-CN method and the rational formula. This model is available as an ArcGIS toolbox, comprising four modules: estimation of the water depth available for runoff, runoff coefficient determination, computation of travel time within the watershed, and a module for discharge estimation (Crăciun, 2011; Gyori, 2013). The workflow for runoff hydrographs determination consists of the aforementioned incorporated modules, a step for flow velocity computation in SAGA GIS and 5 scripts created by Domnița (2012) in MATLAB (Gyori, 2013). The current research is based only on the NRCS-CN method for discharge estimation, similarly to the approach of Haidu and Strapazan (2019). The computation of surface runoff for each grid cell, in this case, involved the same equation embedded in the model implemented by Crăciun (2011), which accounts for the cumulative water infiltration (Musy & Higy, 1998):

$$Q = P - I_a - F \tag{15}$$

Where:

Q – runoff (mm);

P – rainfall (mm);

I_a – initial abstractions (mm);

F – cumulative infiltration (mm).

The model was subsequently upgraded by including the effect of slope on the cumulative infiltration (Crăciun, 2011):

$$F = \frac{S \cdot (P - I_a)}{P - I_a + S} \cdot (1 - Ib / 100) \tag{16}$$

Unde:

Ib – slope (degrees).

The only tool that most GIS products lack is the one able to compute the overland and channel flow velocity, which is why the original model/procedure relies on the *Isochrones Variable Speed* algorithm available in SAGA GIS for this stage (Domnița, 2012). This research used MATLAB v.9.14.0 (R2023a) Update 2, under a DEMO/Trial license obtained from the MathWorks Inc. website (The MathWorks Inc., 2023), in order to run the abovementioned scripts. In this case, a new GIS-based flow velocity calculation algorithm was implemented in ArcGIS 10, and the CN values were calibrated using another algorithm specifically developed for this purpose. The flowchart methodology used, associated with this particular research can be observed in Figure 9.

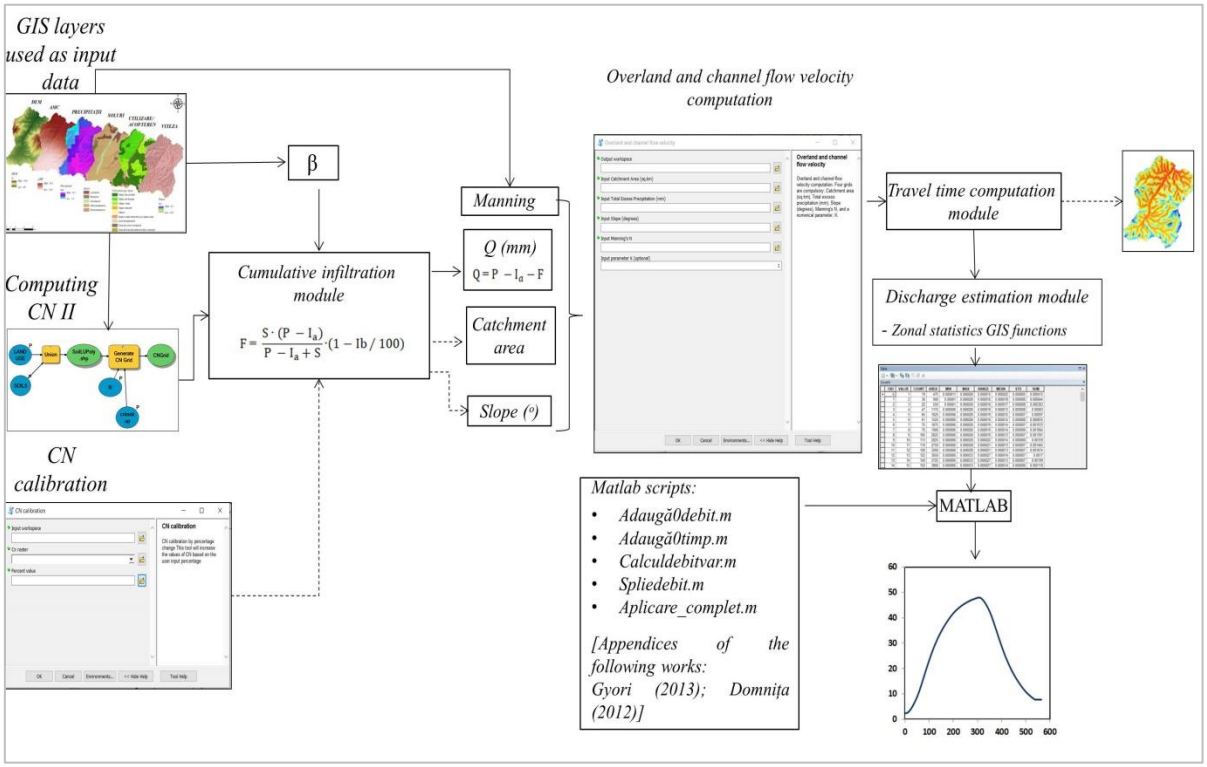

Figure 9. Overview of the workflow used in this study for flood events simulation with the Cluj Model

5.5.1. Implementation of a Python-based GIS algorithm for flow velocity estimation

When a hydrologic model workflow involves several processes such as the transfer of data between various software packages, not only are errors frequent and the process is time-consuming, but sometimes it becomes quite challenging and unintelligible. Therefore, another objective of the present research was the implementation of a new GIS-based algorithm for overland and channel flow velocity estimation through Python scripting and the ArcPy package.

The equation for the overland flow velocity estimation is similar to that embedded in SAGA GIS and is based on the combination of kinematic wave approximation with Manning's equation (Al-Smadi, 1998; Olaya, 2004a, 2004b):

$$V_o = \frac{(i_e \cdot x)^{0.4} \cdot S_o^{0.3}}{n^{0.6}} \quad (17)$$

Unde:

V_o – overland flow velocity (m/s);

i_e – excess rainfall intensity (m/s);

n – Manning's roughness coefficient;

S – surface slope (m/m);

x – distance along the flow plane (m).

Concerning the channel flow velocity estimation, the applied method in this case, is based on the combination of Manning's equation with the continuity one, as follows (Du et al., 2009; Tsanakas et al., 2016):

$$V_c = K \cdot S_o^{3/8} \cdot Q_{ch}^{1/4} \cdot n^{-3/4} \quad (34)$$

Unde:

V_c – channel flow velocity (m/s);

K– coefficient that is determined through calibration;

S – surface slope (m/m);

Q_{ch} – discharge (m^3/s);

n – Manning's roughness coefficient.

Therefore, a standalone Python script was created and initially run for verification and validation from PyScripter. Subsequently, it was converted into an ArcGIS tool that can be easily accessible to anyone interested in using the distributed-parameter model (Figure 10).

The required input data for the application are: the excess precipitation (mm/h), catchment area (km^2), slope (degrees), Manning's n and K.

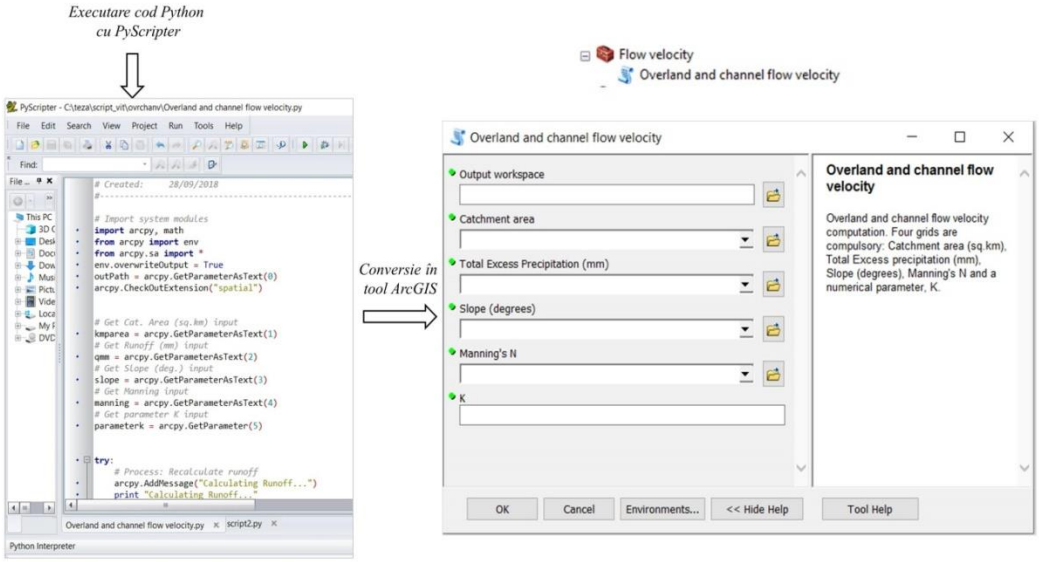

Figure 10. Running the script from PyScripter and the graphical interface of the GIS tool for overland and channel flow velocity estimation

5.5.2. Implementation of a GIS algorithm for CN parameter calibration

The main purpose of applying this distributed model was to evaluate its utility in estimating flood hydrographs in comparison to the results provided by the lumped-parameter one. Additionally, the application of this model served the secondary purpose of determining its compatibility with the GIS-based flow velocity algorithm. Thus, the procedure followed in this case is closely related to the results generated by the lumped model and it was performed subsequent to the first one.

In this context, relying on the hypothesis that better results in reproducing flood hydrographs could be achieved with CN values determined based on the rainfall-runoff relationship, a GIS algorithm was implemented in order to calibrate those values obtained from the cumulative infiltration module. The algorithm, in this case, is a much simpler one, involving the percentage change in CN values and the creation of new layers related to CN and S values in order to generate a calibrated cumulative infiltration. The implementation of this algorithm was carried out through a script created in a similar manner to the one used for computing flow velocities. Even though it involves straightforward calculations, a script file

creation and subsequent conversion into a GIS tool automate the process, thus reducing the time-consuming process of calibration and determination of the new S values (Figure 11).

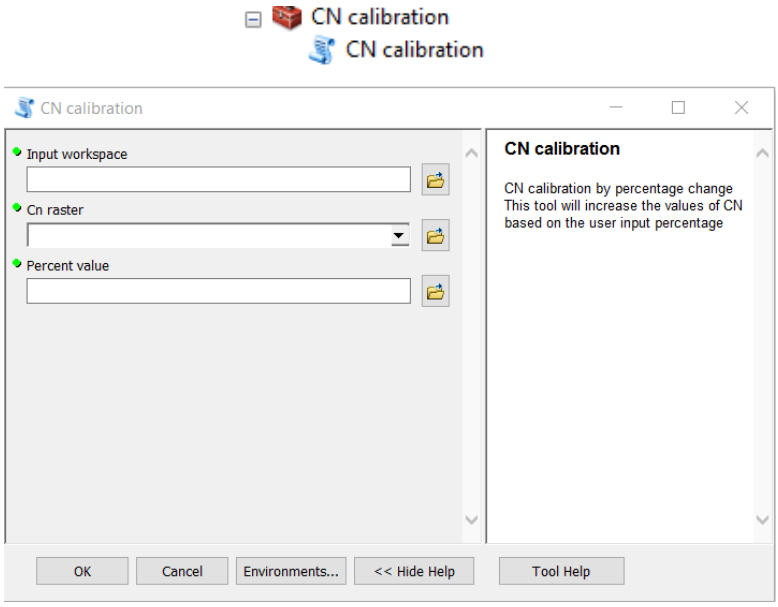

Figure 11. The graphical interface of the GIS tool for CN calibration

6. RESEARCH RESULTS AND DISCUSSION

6.1. Applications to determine CN values. Comparative approach between the traditional procedure and the one based on the rainfall-runoff relationship

Tables 3 and 4 list the representative CN values for each study watershed derived from the adapted NEH630 tables to the territorial features of our country and the ones determined by the rainfall-runoff data-based methods both for $\lambda = 0.2$ and $\lambda = 0.05$. The values estimated by the central tendency methods were generally higher than in the other cases, with CN-AM values (determined using the AM method) lower than those of GM, but higher than CN-MD (corresponding to the MD method) for 2 out of the 4 study basins (Timiș and Ozunca), using both $\lambda = 0.2$ and $\lambda = 0.05$, similar results being reported by Tedela et al. (2012) for 4 out of the 10 forested watersheds located in the eastern U.S. (Strapazan et al., 2023a).

The CN-TAB values (corresponding to the TAB method) vary between 50.00 (Timiș watershed) and 73.00 (Ozunca watershed), with Timiș having the highest forest coverage (92.4%) and Ozunca the lowest (55.5%). Moreover, the CN values computed based on the central tendencies do not show significant differences among basins or methods, but when compared to those obtained through the TAB method, they are significantly higher, a general

similarity between the central tendencies being also reported by Im et al. (2020) for 6 experimental forested basins from South Korea and Japan.

Table 3. CN values derived by different methods for λ = 0.2 (after Strapazan et al., 2023a)

Watershed	MD	GM	AM	AF_O		AF_N		Behavior	TAB
				CN_{AFo} (R^2, SE)	k (SE)	CN_{AFn} (R^2, SE)	k (SE)		
Teliu	85.85	85.89	85.06	80.45 (0.94, 0.438)	0.034 (0.002)	70.00 (0.43, 7.228)	0.017 (0.007)	Standard	54.00
Timiș	76.52	79.55	77.99	71.98 (0.88, 0.442)	0.038 (0.002)	68.91 (0.51, 2.081)	0.029 (0.005)	Standard	50.00
Ozunca	83.12	84.29	83.69	79.58 (0.80, 0.664)	0.049 (0.004)	73.90 (0.43, 4.970)	0.030 (0.011)	Standard	73.00
Covasna	82.56	83.98	83.45	81.87 (0.23 0.883)	0.050 (0.011)	79.77 (0.19 2.311)	0.034 (0.011)	Standard	61.00

Table 4. CN values derived by different methods for λ = 0.05 (after Strapazan et al., 2023a)

Watershed	MD	GM	AM	AF_O		AF_N		Behavior	TAB
				CN_{AFo} (R^2, SE)	k (SE)	CN_{AFn} (R^2, SE)	k (SE)		
Teliu	80.88	80.89	79.81	75.61 (0.89, 0.524)	0.046 (0.003)	64.18 (0.33 7.504)	0.022 (0.009)	Standard	39.03
Timiș	66.96	71.43	69.67	63.91 (0.64, 0.476)	0.066 (0.005)	59.55 (0.30, 2.697)	0.042 (0.009)	Standard	34.74
Ozunca	75.27	77.19	76.36	73.84 (0.29, 0.687)	0.092 (0.013)	66.51 (0.24, 5.890)	0.042 (0.017)	Standard	62.56
Covasna	79.04	78.97	78.23	77.09 (0.03, 0.810)	0.103 (0.051)	75.26 (0.054, 2.470)	0.053 (0.025)	Standard	47.10

The analysis of the results obtained through the AF method reveals standard behavioral patterns on all of the 4 studied watersheds, showing consistent trends, especially in the case of ordered data series (Figure 12). However, this situation is also characteristic for the unordered series both for λ = 0.2 and 0.05 (Figure 13). This type of behavior seems to be the general pattern in various geographical locations around the world, present findings being consistent with results from other studies such as Hawkins (1993), Tedela et al. (2012), D'Asaro et al. (2014), Kowalik and Walega (2015), Ajmal et al. (2016), which found the same response on most of the studied basins.

Regarding the runoff estimation results based on CNs determined by the abovementioned methods, the statistical indicators revealed once again the similarity of the central tendency methods.

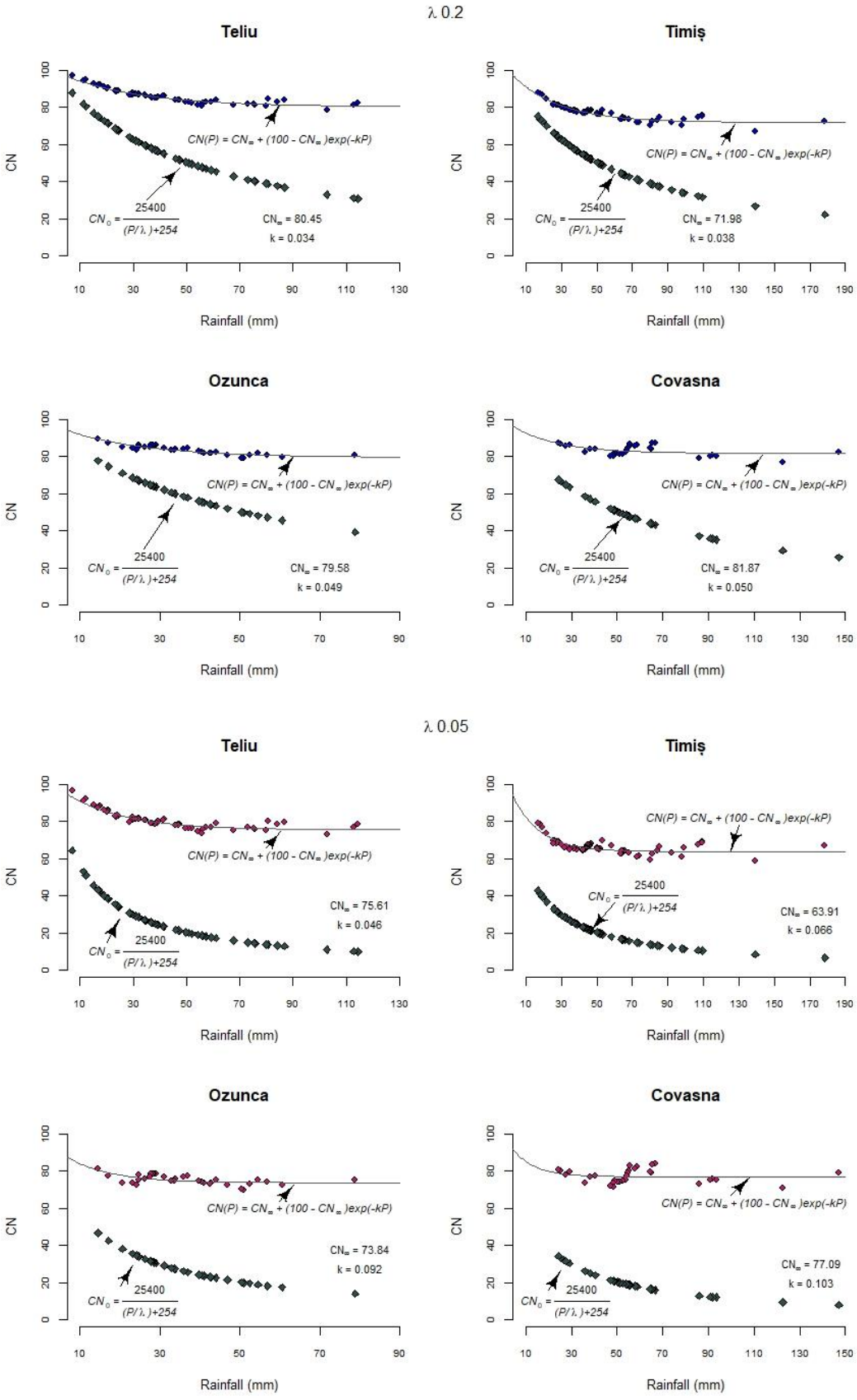

Figure 12. CN-AF$_O$, namely the curve number values determined by the asymptotic fitting method for the rank-ordered P-Q data pairs, using both values of 0.2 and 0.05 for λ (modified after Strapazan et al., 2023a)

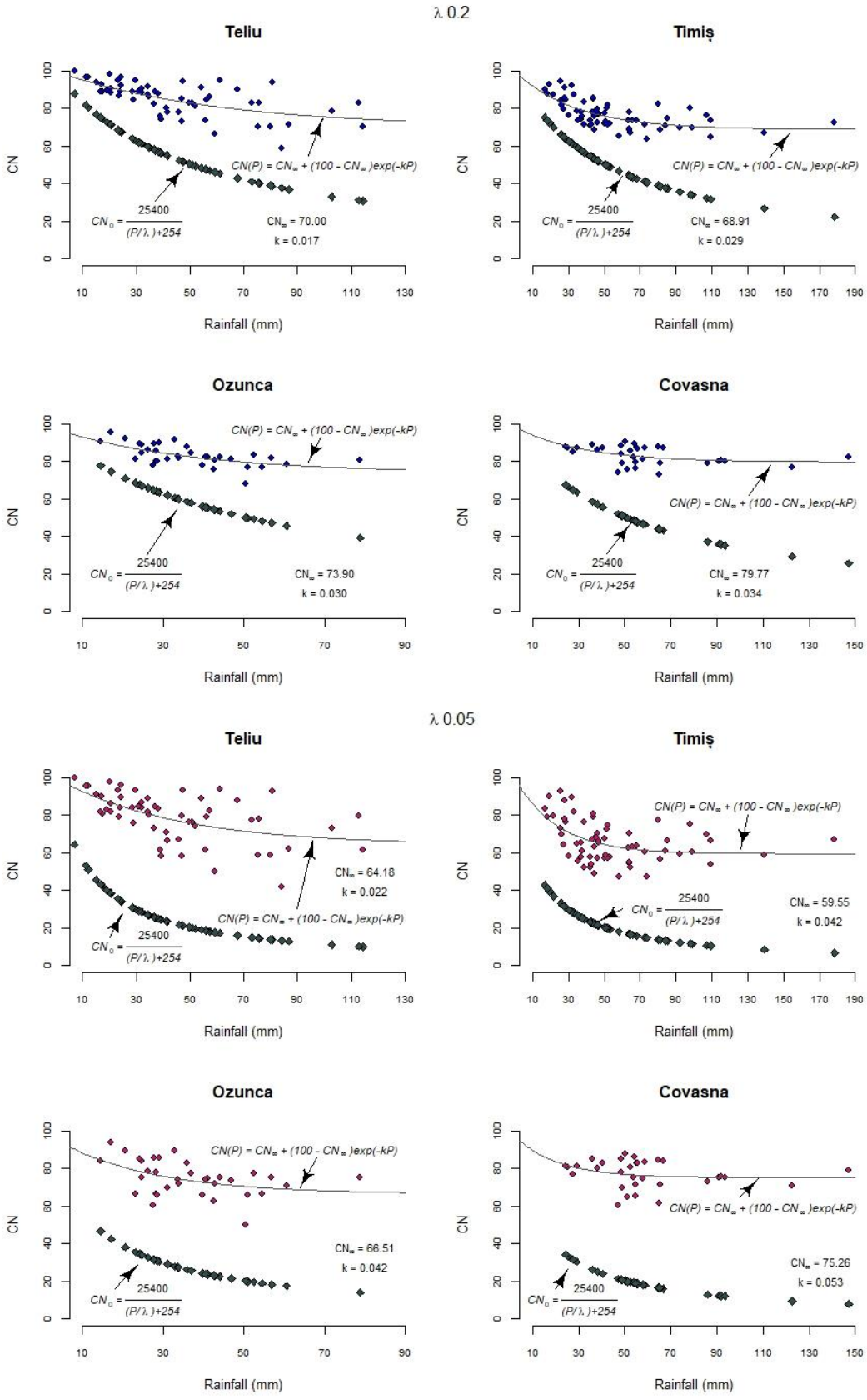

Figure 13. CN-AF$_N$, namely the curve number values determined by the asymptotic fitting method for the natural sorting of P-Q data pairs, using both values of 0.2 and 0.05 for λ (modified after Strapazan et al., 2023a)

The boxplot or "box and whisker" plot (Figure 14) also reveals a similar distribution pattern of values derived from the central tendency methods with the smallest range of values belonging to the TAB method. Considering the criteria recommended by Moriasi et al. (2007), it was observed that in most cases, the models achieved satisfactory results given the *NSE* and R^2 > 0.50, with the exception of the TAB and AF_N methods, which exhibit the highest *RMSE* values and, in almost all cases, *PBIAS* values that do not fall within the ±25% range. If the results are analyzed following the criteria recommended by Diaz-Ramirez et al. (2011), it is undeniable that the performance of the central tendency methods is good for Teliu and Ozunca, and very good for Timiș and Covasna watersheds. Although the study highlighted the similarity of results obtained through the application of central tendency methods and the comparable ones associated with the AF_O method, there are slight differences, given that more accurate results were achieved for λ = 0.05, with the MD method for the larger watersheds, and the AM one for those with smaller drainage areas (Strapazan et al., 2023a).

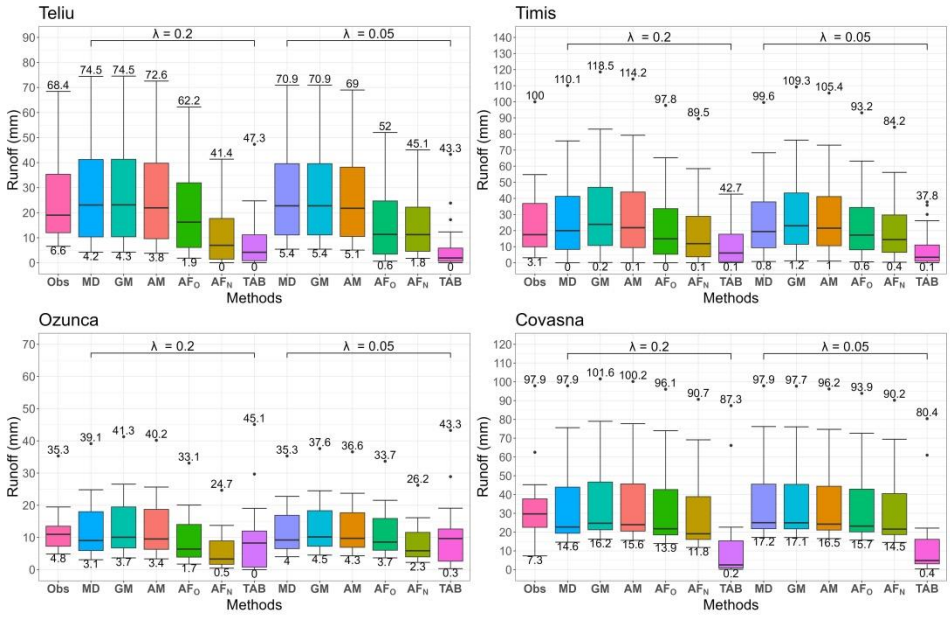

Figure 14. Boxplots displaying the distribution of estimated runoff between the methods MD, GM, AM, AF_O, AF_N și TAB employed and the measured runoff (Obs) for λ = 0.2 and λ = 0.05 (modified after Strapazan et al., 2023a).

Following the previously undertaken study, we proceeded with the analysis of the complete dataset to investigate whether the distribution of events could be determined based on CN percentiles. These analyses were carried out for the results corresponding to λ = 0.2. In this case, the classification was directly performed based on CN percentiles and the resulting

R^2 values for each class. Events for which $P < 25.4$ mm and $P/S < 0.46$ were excluded from the dataset. The classification that yielded the highest R^2 values for Teliu and Covasna corresponds to the 80th and 20th CN percentiles, while in the case of Timiș and Ozunca, the classification was based on the 78th and 22th CN percentiles, which were considered the actual thresholds for AMC III and I.

6.2. Rainfall spatialization using radar information and field-measured data.

A series of radar-based rainfall data provided by the weather radar located at Bobohalma were used. Specifically, the aim was to calibrate the lag time within the simulation processes of flood hydrographs corresponding to the growing season, based on the available data. The hypothesis was that the estimation of the best values for certain parameters (the lag time in this case, since the CN values were determined as discussed earlier) for flood events modeling can only be achieved using high spatial and temporal resolution rainfall data (3-hours or even hourly rainfall accumulation data). Subsequently, the same data were used to run the distributed-parameter model for flood hydrographs estimation. Hourly accumulations as mean values of classes associated with the radar algorithm were further processed to match the frequency of station records, aiming to process and correct the radar estimates based on rain gauge data. The evaluation and verification of the adjusted radar-rainfall field was performed based on R^2 values ranging from 0.90 to 0.98 within the study area (Table 5).

Table 5. Data used for the radar-rainfall correction procedure

Watershed	Weather stations	Hydrometric stations	Date	Rainfall accumulations	R^2
Teliu	Întorsura Buzăului	Teliu	29.06-01.07.2018	3, 6, 12 h	0.97
Timiș	Predeal, Vf. Omu, Brașov-Ghimbav	Dâmbu Morii, Râșnov, Babarunca	01-03 08.2010	24 h	0.98
Ozunca	Miercurea Ciuc	Bățanii Mari, Micfalău	07-08.05 2005	12 h	0.90
Covasna	Întorsura Buzăului, Târgu Secuiesc, Sfântu Gheorghe, Lăcăuți	Covasna	01-03.08 2010	12 h	0.90

6.3. Comparative assessment of different methods available in MIKE HYDRO River-UHM with applications in the Teliu watershed.

The first part of the study addressing the applicability of the UHM-MIKE HYDRO River module, involves a comparative analysis of the NRCS-CN (SCS), SCS generalised, and Proportional loss methods available, carried out in a small mountainous basin, for which no such studies have been conducted before. Among the study watersheds, Teliu is the smallest one and is located within an area with a low density of monitoring sections, thus making it a suitable case study in this context. Three runoff events were selected for model calibration and validation, considering the rainfall and runoff seasonality in this area (heavy spring rainfall events during April-May) and their magnitude, with water levels exceeding the predetermined threshold for issuing warnings (H = 100 cm), being among the highest events on the historical analyzed record. The AMC (established according to the traditional NRCS-CN procedure) for the 2016 event used for model calibration (AMC I) differs from that of the other two events in 2012 selected for validation (AMC III). In order to apply the SCS method, initial computations were based on the classical NRCS-CN procedure to determine CN and T_{lag} values, and the λ coefficient required by the SCS generalised method was established through calibration, taking values that varied between 20 mm (30% of S) to 15 mm (corresponding to 23% of S). In order to apply the Proportional loss method, the estimation and the spatial distribution of the runoff coefficient were automatically performed using Frevert indices within a GIS-based model developed by Crăciun (2011), and the resulting values range between 0.12 and 0.45 for the drainage area. The performance evaluation was conducted based on several statistical indicators such as *RMSE*, R^2, *PEP*, *NSE*, and *d* (Table 6). Upon analyzing the measured data, it was observed that a lag time value in the range 8 to 12 hours would be appropriate, considering that about 12 hours have passed from the centroid of rainfall excess to the peak runoff occurrence. The obtained results were surprisingly good, and finally, a T_{lag} of 10 hours and CN = 79, corresponding to AMC II, were identified as the most appropriate parameters in the given situation (Strapazan et al., 2021). The CN value obtained through calibration in this case is similar to the one determined by the AF_O method and relatively close to the CN values determined by the central tendency methods based on measured data during the growing season (Strapazan et al., 2023a). Accurate peak discharge time estimates were also noticed. For the April 2012 event, the best results were achieved with the SCS method (Table 7).

Table 6. Statistics for different parameter values and loss methods used for calibration for the runoff event on April 2016 (modified after după Strapazan et al., 2021)

Metode utilizate	**Parametri**	***RMSE***	***R^2***	***NSE***	***d***
SCS	CN=54-80 *AMC inițial=I* *T_{lag} derivat=1.19-2.32*	4.66-6.64	0.14-0.41	<0.00	0.47-0.70
	CN=54-80 *AMC=II* *T_{lag} derivat=1.15-2.32*	5.28-7.90	0.12-0.47	<0.00-0.07	0.50-0.60
	CN=67-80 *AMC=II* *T_{lag} definit=8-12*	1.74-4.23	0.87-0.94	<0.00-0.88	0.70-0.96
	Final: *CN=79, AMC=II,* *T_{lag} definit=10*	1.77	0.94	0.87	0.96
SCS generalised	CN=79 *λ inițial=15-20* *T_{lag} definit=10*	0.18-2.21	0.87-0.91	0.84-0.86	0.95
	CN=79 *λ =15-20* *T_{lag} definit=9*	2.11-2.24	0.9-0.92	0.86	0.95
	Final: *CN=79, λ=16, T_{lag} definit=9*	2.20	0.92	0.86	0.95
Proportional loss	α=0.36-0.50 *T_{lag} definit=10*	2.09-2.45	0.87	0.75-0.85	0.94-0.95
	α=0.36-0.50 *T_{lag} definit=12*	1.42-1.78	0.94	0.81-0.92	0.96-0.98
	Final: *α=0.45* *T_{lag} definit=12*	1.42	0.94	0.92	0.98

Table 7. Validation and statistical evaluation results for the runoff events on April and May, 2012 (modified after Strapazan et al., 2021)

Metode utilizate	**Data**	***RMSE***	***R^2***	***NSE***	***d***
SCS	18-21.04.2012	0.93	0.89	0.85	0.95
	29-31.05.2012	1.47	0.73	0.68	0.88
SCS generalised	18-21.04.2012	0.90	0.88	0.62	0.93
	29-31.05.2012	1.58	0.38	0.05	0.76
Proportional loss	18-21.04.2012	1.21	0.68	0.61	0.90
	29-31.05.2012	1.16	0.77	0.72	0.91

Although the Proportional Loss method yielded the best results for the 2016 and May 2012 events, the hydrograph shape was best reproduced by the SCS method (Figure 15).

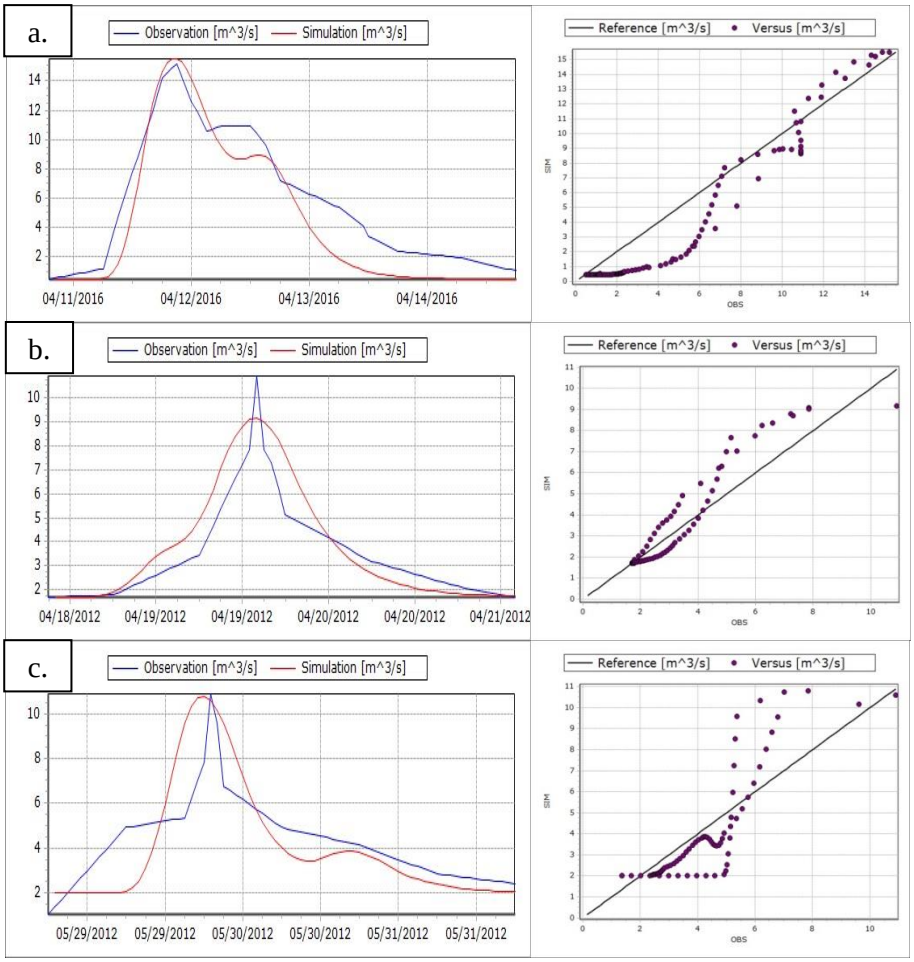

Figure 15. Comparison between the measured and estimated runoff hydrographs with the SCS method for the: a) 2016, b) April 2012 and c) May 2012 events (adaptare după Strapazan et al., 2021)

6.4. Application of the SCS method available in the MIKE HYDRO River-UHM and results. Comparative assessment of CN values computed for the growing season

The main purpose in this case was to analyze, apply, and validate the MIKE HYDRO River-UHM modeling system through different approaches of the NRCS-CN method. The applications were carried out on all the study watersheds. The applicability of the method for various AMC conditions has been demonstrated based on several of the largest events that occurred in the Teliu watershed. Considering that acceptable results were achieved only through calibration and that they were superior to those generated by other methods, the present research relies solely on the abovementioned method. In other words, the research aims to validate, through flood hydrograph simulations, the CN values determined not only through the tabular NRCS-CN method (TAB) but also based on the rainfall-runoff relationship by the central tendency methods and AF_O.

In this case, a total of 19 events were chosen. For each watershed, those CN values determined by the central tendency methods, that provided optimal results for $\lambda = 0.2$ with regard to surface runoff estimation were selected, considering the classical procedure embedded in MIKE HYDRO River-UHM. Regarding the radar data and its availability, one representative rainfall event was chosen for each basin and flood hydrographs simulations were performed in order to establish the lag time based on the adjusted radar-rainfall field.

Teliu River basin

A total of 11 events were selected in order to calibrate and validate the model based on the NRCS-CN method (which we will refer to as SCS, as it is designated within the modeling system). The highest peak discharges were considered for the selection process (the largest flood events with available information) along with available past weather warnings data and information related to the rainfall intensity and duration from the m.s. Întorsura Buzăului. The events from the previous subchapter were revisited here for comparative purposes.

The first step involved the flood hydrographs simulation based on the classical SCS procedure, by classifying the events according to AMC5 conditions (based on the 5-day antecedent rainfall depth). However, instances occurred when simulation could not be performed for certain AMC classes (e.g., 08-11.08.2010, 06-10.05.2019, 20-23.09.2005, etc.), which required the conversion of CN values to other conditions, taking into account the classification based on CN percentiles and the possibility that the measured rainfall may not entirely correspond to the actual field situation. Much better results were thus obtained, though with $NSE < 0$, a common situation for all the analyzed events, except for those in 2018 and 2010.

Although the 2018 flood event simulation was performed by using gauge-corrected radar-based estimates, the *NSE* remained below the acceptable threshold value (Table 8). Considering the best results obtained through the traditional procedure (mainly corresponding to AMC III), it was observed that, in most cases, the lag time should be much greater than 2 hours, with the exception of the 29.06-01.07.2018 and 20-22.06.2020 events.

Differences of more than 4 hours were noticed between the computed and measured peak flow times for 7 out of 11 cases. In the next step, T_{lag} calibration was performed on the 2018 (for which radar data was available), 2020, 2012, and 1991 events.

Table 8. Results of the simulations based on the SCS method for CN-TAB = 54 and T_{lag} derived for different AMC

Eveniment	AMC	Q max măsurat		Q max simulat		Indicatori statistici				
		m^3/s	Moment producere	m^3/s	Moment producere	*PEP (%)*	*RMSE*	R^2	*NSE*	*d*
29.06-01.07. 2018	III	63.0	30.06 – 15:00-16:00	39.4	30.06 – 16:00-	37	8.70	0.57	0.37	0.84
29-03.06. 2014	II	9.3	31.05 - 16:00	3.0	31.05 - 18:00	68	3.4	0.54	<0	0.49
	III	9.3	31.05 - 16:00	9.7	31.05 - 11:00	4	2.85	0.39	<0	0.68
08 - 11.08. 2010	II	10.9	09.08 – 06:00	0.8	09.08 – 06:00	93	4.09	0.64	<0	0.45
	III	10.9	09.08 – 6:00	10.5	09.08 – 2:00	4	2.33	0.73	0.44	0.84
20 - 23.09. 2005	II	8.1	21.09 – 06:00	0.37	21.09 – 9:00	95	3.75	0.22	<0	0.43
	III	8.1	21.09 – 06:00	7.95	21.09 – 0:00	1	3.34	0.07	<0	0.52
06-10.05. 2019	III	6.4	07.05 – 09:00	5.56	07.05 – 7:00	13	2.18	0.15	<0	0.49
12-15.06. 2020	II	15.9	12.06 – 6:00	0.8	13.06 – 7:00	95	4.82	0.23	<0	0.45
	III	15.9	12.06 – 6:00	10.7	12.06 – 5:00	33	3.46	0.64	<0	0.73
20-22.06. 2020	III	7.6	20.06 – 12:00	4.2	20.06 – 14:00	44	2.2	0.46	<0	0.59
26-30.05. 1991	I	42.7	27.05 – 12:00	8.55	28.05 – 23:00	80	13.52	0.01	<0	0.46
	II	42.7	27.05 – 12:00	9.6	27.05 – 7:00	77	13.34	0.06	<0	0.46
	III	42.7	27.05 – 12:00	27.7	27.05 – 7:00	35	12.12	0.16	<0	0.53
11-14.04. 2016	III	15.2	11.04 – 21:00	23.8	11.04 – 11:00	57	6.03	0.15	<0	0.60
29-31.05. 2012	III	10.9	29.05 – 19:00	4.8	29.05 – 11:00	56	2.70	0.07	<0	0.47
18-21.04. 2012	III	10.9	19.04 – 14:00	3.72	19.04 – 9:00	66	2.31	0.14	<0	0.49

The computed T_{lag} values varied significantly among the events, leading to the determination of an average value of about 6.8 hours for utilization. This value is the one that resulted through calibration based solely on the 2018 data when the most extreme event ever recorded took place (since the establishment of the monitoring station in 1987). The results were surprisingly good, with maximum time differences of 4 hours between the observed and the simulated peak discharge. The calibration and validation stages resulted in R^2 values ranging from 0.36 to 0.94 for CN = 85 and from 0.35 to 0.94 for CN = 80 (Tables 9-12), much better than those from Table 8. Only one situation with *RMSE* > 10 was identified, corresponding to the 2018 event (Figure 16), and larger errors were observed for the simulations based on CN = 85.

Table 9. Results of the simulations based on the SCS method and the input parameters for UHM - MIKE Hydro River. Calibration phase with CN-AM = 85

Event	Observed peak flow		Simulated peak flow			Statistical indicators				
	m^3/s	Time of peak	m^3/s	Time of peak	T_{lag}	*PEP (%)*	*RMSE*	R^2	*NSE*	*d*
29.06-01.07. 2018	63	30.06 – 15:00-16:00	53.5	30.06 – 15:00	6.8	15	12.08	0.62	0.53	0.82
12-15.06. 2020	15.9	12.06 – 6:00	20.0	12.06 –6:00	4	26	1.94	0.88	0.84	0.95
20-22.06. 2020	7.6	20.06 – 12:00	13.9	20.06 – 14:00	3	83	2.38	0.58	0.51	0.77
26-30.05. 1991	42.7	27.05 – 12:00	42.3	27.05 – 08:00	4	1	7.98	0.36	<0	0.75
11-14.04. 2016	15.2	11.04 - 21:00	20.8	11.04 – 20:00	10	37	2.60	0.94	0.84	0.94
29-31.05. 2012	10.9	29.05 – 19:00	13.6	29.05 – 18:00	10	25	2.22	0.73	0.58	0.81
18-21.04. 2012	10.9	19.04 – 14:00	11.0	19.04 – 14:00	10	1	1.75	0.85	0.66	0.87

Table 10. Results of the simulations based on the SCS method and the input parameters for UHM - MIKE Hydro River. Validation phase with CN-AM = 85

Event	Observed peak flow		Simulated peak flow			Statistical indicators				
	m^3/s	Time of peak	m^3/s	Time of peak	T_{lag}	*PEP (%)*	*RMSE*	R^2	*NSE*	*d*
08-11.08. 2010	10.9	09.08 – 6:00	16.9	09.08 – 7:00	6.8	55	3.40	0.84	0.62	0.82
29.05-03.06. 2014	9.3	31.05 – 16:00	12.2	31.05 – 14:00	6.8	31	2.37	0.75	0.60	0.83
20-23.09. 2005	8.1	21.09 – 06:00	11.8	21.09 – 03:00	6.8	47	2.47	0.84	0.65	0.84
06-10.05. 2019	6.4	07.05 – 09:00	9.7	07.05 – 09:00	6.8	52	1.76	0.72	0.50	0.78

Table 11. Results of the simulations based on the SCS method and the input parameters for UHM - MIKE Hydro River. Calibration phase with CN-AF_O = 80.45

Event	Observed peak flow		Simulated peak flow			Statistical indicators				
	m^3/s	Time of peak	m^3/s	Time of peak	T_{lag}	*PEP (%)*	*RMSE*	R^2	*NSE*	*d*
29.06-01.07.2018	63.0	30.06 – 15:00-16:00	49.04	30.06 – 16:00	6.8	22	10.54	0.62	0.57	0.85
12-15.06.2020	15.9	12.06 – 06:00	14.9	12.06 – 06:00	4	6	1.97	0.84	0.68	0.93
20-22.06.2020	7.6	20.06 – 12:00	8.5	20.06 – 14:00	3	13	1.79	0.52	0.17	0.78
26-30.05.1991	42.7	27.05 – 12:00	39.5	27.05 – 08:00	4	8	8.46	0.35	<0	0.73
11-14.04.2016	15.2	11.04 – 21:00	16.3	11.04 – 20:00	10	7	1.78	0.94	0.88	0.96
29-31.05. 2012	10.9	29.05 – 19:00	10.81	29.05 – 18:00	10	1	1.47	0.73	0.68	0.88
18-21.04.2012	10.9	19.04 – 14:00	9.2	19.04 – 14:00	10	16	0.93	0.89	0.85	0.95

Satisfactory or even strong correlations were detected in most cases with relatively acceptable errors, but for the much higher CN values (compared to those determined following the classical procedure). Thus, the CN-AF_O values, although slightly inferior to those associated with the central tendencies in estimating the runoff depth (Strapazan et al., 2023), in this case resulted in much smaller errors compared to those related to the CN-AM (except for the 2018 and 1991 events).

Tabel 12. Results of the simulations based on the SCS method and the input parameters for UHM - MIKE Hydro River. Validation phase with CN-AF$_O$ = 80.45

Event	Observed peak flow		Simulated peak flow			Statistical indicators				
	m^3/s	**Time of peak**	**m^3/s**	**Time of peak**	**T$_{lag}$**	***PEP (%)***	***RMSE***	***R^2***	***NSE***	***d***
08-11.08.2010	10.9	09.08 – 06:00	12.0	09.08 – 07:00	6.8	10	1.99	0.80	0.73	0.90
29.05-03.06.2014	9.3	31.05 – 16:00	9.9	31.05 – 15:00	6.8	6	2.05	0.80	0.54	0.85
20-23.09. 2005	8.1	21.09 – 06:00	8.8	21.09 – 03:00	6.8	10	1.62	0.85	0.70	0.90
06-10.05.2019	6.4	07.05 – 09:00	6.4	07.05 – 10:00	6.8	0	1.55	0.74	0.07	0.76

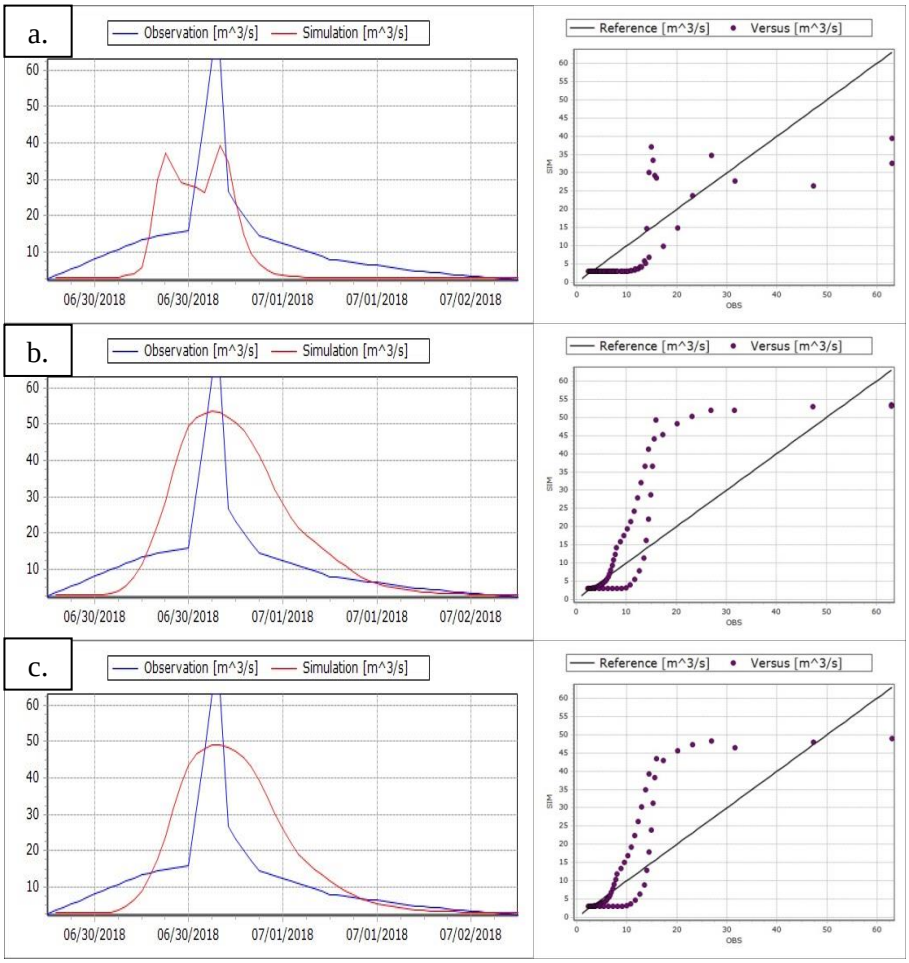

Figure 16. Comparison between the measured and estimated runoff hydrographs for the Teliu watershed based on: a. CN-TAB and computed T$_{lag}$; b. CN-AM and defined T$_{lag}$; c. CN-AF$_O$ and defined Tlag.

Timiș River basin

From the available dataset for the Timiș watershed, the largest events recorded during the growing season took place in 1994 (June), 2001 (September), 2010 (August), and 2010 (July). Regarding the other years, significant flood events occurred mainly before 2009, and the used databases lack of high-frequency precipitation records from m.s. Predeal. In light of

this and the m.s. Predeal's influence over a large area within the watershed, this study case will rely only on the flood events recorded during July and August, 2010. The first simulations were performed for the August, 2010 flood event based on gauge-corrected radar-based information. The simulation process for the July, 2010 flood event with CN-TAB (50) did not yield any results for AMC III conditions. The outcomes were unsatisfactory for the August, 2010 event (Table 13). The best results were achieved with CN-MD, instead (Table 14). This is shown by most of the points which are clustered around the reference line, and the relatively small error of 16% in peak flow estimation. For CN-AF_O (Table 15), the *PEP* value reached 54%, suggesting the general tendency for discharge underestimation. However, much better results were achieved compared to the previous situation, but in this case, the T_{lag} calculated according to the classical procedure provided optimal results, eliminating the need for calibration.

Tabelul 13. Results of the simulations based on the SCS method for CN-TAB = 50 and automatically derived T_{lag}.

Event	AMC	Observed peak flow		Simulated peak flow			Statistical indicators				
		m^3/s	Time of peak	m^3/s	Time of peak	T_{lag}	*PEP (%)*	*RMSE*	R^2	*NSE*	*d*
01-02.08.2010	III	45.8	01.08 -20:30	11.8	01.08 – 23:00	2.93	74	9.42	0.37	<0	0.53
14-15.07.2010	III	Fără rezultat									

Table 14. Results of the simulations based on the SCS method for CN-MD = 76.5 and automatically derived T_{lag}.

Event	Observed peak flow		Simulated peak flow			Statistical indicators				
	m^3/s	Time of peak	m^3/s	Time of peak	T_{lag}	*PEP (%)*	*RMSE*	R^2	*NSE*	*d*
01-02.08.2010	45.8	01.08 -20:30	38.7	01.08 – 21:00	1.44	16	4.31	0.88	0.78	0.95
14-15.07.2010	36.6	14.07 – 20:30	47.8	14.07 – 21:30	1.44	31	11.16	0.72	0.40	0.79

Tabelul 15. Results of the simulations based on the SCS method for CN-AF_O = 72 and automatically derived T_{lag}.

Event	Observed peak flow		Simulated peak flow			Statistical indicators				
	m^3/s	Time of peak	m^3/s	Time of peak	T_{lag}	*PEP (%)*	*RMSE*	R^2	*NSE*	*d*
01-02.08.2010	45.8	01.08 -20:30	20.9	01.08 – 21:30	1.66	54	7.23	0.76	<0	0.76
14-15.07.2010	36.6	14.07 – 20:30	29.5	14.07 – 22:00	1.66	19	12.01	0.61	<0	0.69

Ozunca River basin

From the available dataset, those that occurred in 2005 (May)- for which radar data was available for T_{lag} calibration, 2016 (June), and 2010 (June) events were selected. On June 28, 2016, the most extreme event ever recorded took place (since the station's establishment in 1979). As in other cases, the simulation process did not yield any results for the 2005 (Figure 21) and 2016 events with AMC5. Overall, the method's performance employing CN-TAB

was unsatisfactory (Table 16) considering the low R^2 value for the 2016 event, and the quite large errors associated (*RMSE* = 23.81). For the other cases, the performance was relatively satisfactory or even good (e.g. 2005), but with low *NSE* values. Although the simulation results based on the CNs determined by the central tendency methods did not show major differences among the statistical indicators' values such as *NSE*, R^2, or *d* (Tables 17 and 18), the peak flow values were greatly influenced by these modifications. Optimum results were achieved with CN-AF_O for the 2005 and 2010 events (Figure 17), whereas for the one recorded in 2016, CN-MD yielded the best outcomes. This situation is similar to that identified for the Teliu catchment area.

Table 16. Results of the simulations based on the SCS method for CN-TAB= 73 and automatically derived T_{lag}

Event	AMC	Observed peak flow		Simulated peak flow		Statistical indicators				
		m^3/s	Time of peak	m^3/s	Time of peak	*PEP (%)*	*RMSE*	R^2	*NSE*	*d*
07-08.05.2005	II	36.0	07.05 -17:30	24.0	07.05 –18:00	33	6.70	0.80	<0	0.80
25-28.06.2010	II	29.4	26.06 –15:00	24.5	26.06 –15:30	17	8.70	0.51	<0	0.63
	III	29.4	26.06 –15:00	51.3	26.06 –15:30	74	9.20	0.62	0.43	0.76
28-29.06.2016	III	63.5	28.06 –22:30	71.2	29.06 –00:00	12	23.81	0.15	0.02	0.57

Table 17. Results of the simulations based on the SCS method for CN-MD = 83 and defined T_{lag}

Event	Observed peak flow		Simulated peak flow			Statistical indicators				
	m^3/s	Time of peak	m^3/s	Time of peak	T_{lag}	*PEP (%)*	*RMSE*	R^2	*NSE*	*d*
07-08.05.2005	36.0	07.05 -17:30	53.8	07.05 – 17:30	2	50	7.66	0.78	0.68	0.87
25-28.06.2010	29.4	26.06 – 15:00	45.1	26.06 – 15:00	2	53	7.86	0.63	0.33	0.78
28-29.06.2016	63.5	28.06 – 22:30	54.4	28.06 – 23:00	2	14	17.6	0.21	0.10	0.67

Tabel 18. Results of the simulations based on the SCS method for CN-AF_O = 79.6 and defined T_{lag}.

Event	Observed peak flow		Simulated peak flow			Statistical indicators				
	m^3/s	Moment producere	m^3/s	Time of peak	T_{lag}	*PEP (%)*	*RMSE*	R^2	*NSE*	*d*
07-08.05.2005	36.0	07.05 -17:30	44.4	07.05 – 17:30	2	23	6.06	0.80	0.68	0.90
25-28.06.2010	29.4	26.06 – 15:00	38.9	26.06 – 15:00	2	32	7.79	0.60	0.03	0.75
28-29.06.2016	63.5	28.06 – 22:30	41.6	28.06 – 23:00	2	34	15.86	0.20	<0	0.66

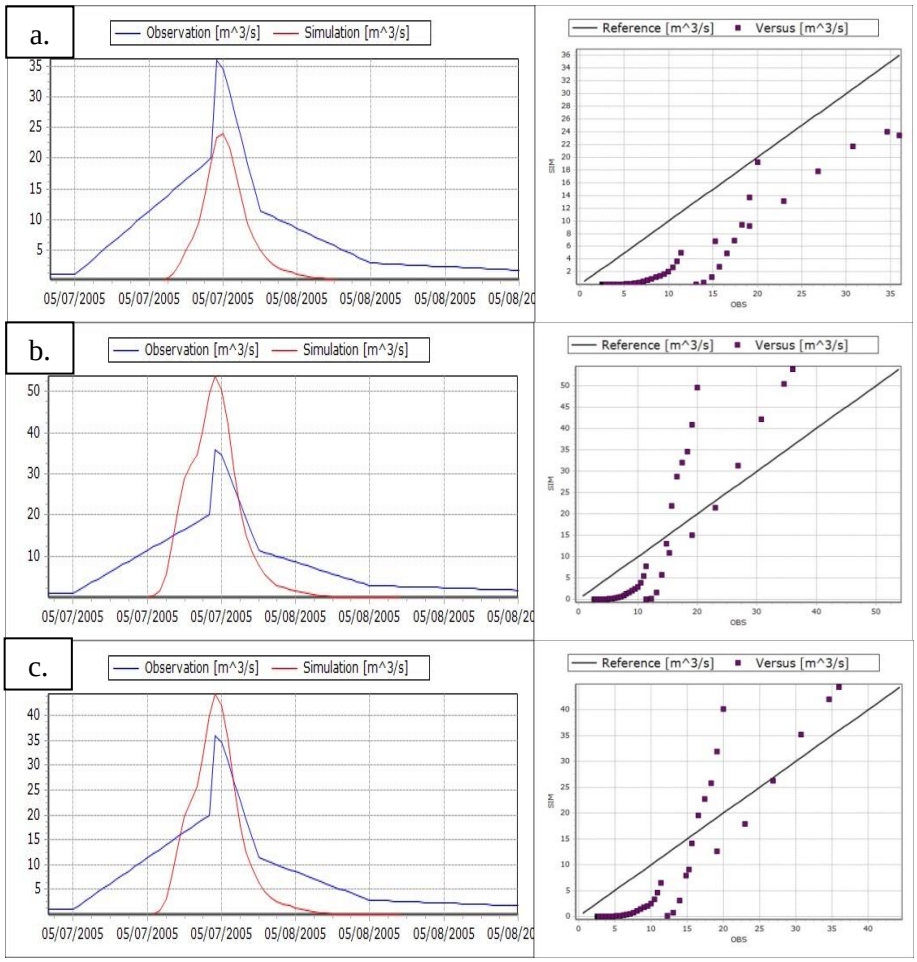

Figure 17. Comparison between the measured and estimated runoff hydrographs at h.s. Bățanii Mari based on: a. CN-TAB and computed T_{lag}; b.CN-MD and defined T_{lag}; c. CN-AF_O and defined T_{lag}

Covasna River basin

For this case study the three largest flood events that occurred during the growing season were selected for the analysis: 2010, 2011, and 2018 events. On August 1st, 2010, the water level exceeded the inundation threshold by 20 cm, making it the most significant event from the available series. Even though radar information was available for this case, the simulation did not yield any results for AMC5, leading to the necessity for AMC II conversion (derived from classifying events based on the 80th and 20th CN percentiles). Nonetheless, the simulated peak flow was by 30% lower than the recorded one. Overall, the errors in peak flow estimation were quite significant for the 2018 and 2010 events, with *PEP* values ranging from 122 to 44%. The method's performance was unsatisfactory for the 2018 event case, with R^2 and *NSE* < 0.5, and satisfactory for the other cases, with R^2 > 0.5 (Table 19).

Considering the similarity between CN-AF_O (81.9) and CN-MD (82.6 with optimal results for λ = 0.2), simulations were performed only for CN-AF_O = 82, taking into account

the better performance of the method for the Teliu watershed (with relatively similar conditional factors). Given the results yielded by the classical SCS approach, a 4 hr T_{lag} was defined. Results showed significantly lower *PEP* and *RMSE* values, and generally higher R^2, *NSE*, and *d* coefficients (Table 20) for the 2018 and 2010 events (Figure 18). In all cases, the method's performance was at least satisfactory for R^2 and *NSE* (except for 2011). This situation resembles the one encountered for the Teliu River basin, where CN-AF_O yielded superior results compared to the classical approach, but for a much higher T_{lag} value than that obtained through the traditional procedure.

In most cases, better simulation results were achieved for CN-AF_O (especially concerning peak flows), supporting Hawkins' theory (1993) regarding the stabilization tendency of CN values towards significant rainfall amounts. Figure 19 illustrates the relationship between peak flow values determined using CN-TAB (selected from the set of optimal results) and those recorded, as well as the relationship between peak flow values (also selected from the optimal results set at the watershed level) determined based on the rainfall-runoff relationship methods (identified as CN-OBS) and those recorded.

Table 19. Results of the simulations based on the SCS method for CN-TAB= 61 and automatically derived T_{lag}

Event	AMC	Observed peak flow		Simulated peak flow		Statistical indicators				
		m^3/s	Time of peak	m^3/s	Time of peak	*PEP (%)*	*RMSE*	R^2	*NSE*	*d*
01-04.08.2010	II	26.1	01.08 – 18:00	7.9	01.08 – 17:00	70	6.53	0.61	<0	0.52
	III	26.1	01.08 – 18:00	37.6	01.08 – 16:00	44	4.98	0.67	0.52	0.85
10-12.06.2011	II	16.0	11.06 -00:00	16.4	10.06 -23:00	2	6.00	0.62	<0	0.68
29.06-03.07. 2018	III	14.0	30.06 –09:00	31.1	30.06 – 06:00	122	5.55	0.29	0.24	0.68

Table 20. Results of the simulations based on the SCS method for CN-AF_O = 82 and defined T_{lag}

Event	Observed peak flow		Simulated peak flow			Statistical indicators				
	m^3/s	Time of peak	m^3/s	Time of peak	T_{lag}	*PEP (%)*	*RMSE*	R^2	*NSE*	*d*
01-04.08.2010	26.1	01.08 – 18:00	31.2	01.08 – 18:00	4	19	4.72	0.65	0.60	0.86
10-12.06. 2011	16.0	11.06 -00:00	18.8	11.06 – 02:00	4	18	5.67	0.66	0.10	0.74
29.06-03.07. 2018	14.0	30.06 –09:00	18.8 (16.9)	01.07 – 00:00 (30.06 – 13:00)	4	34 (21)	2.87	0.74	0.68	0.90

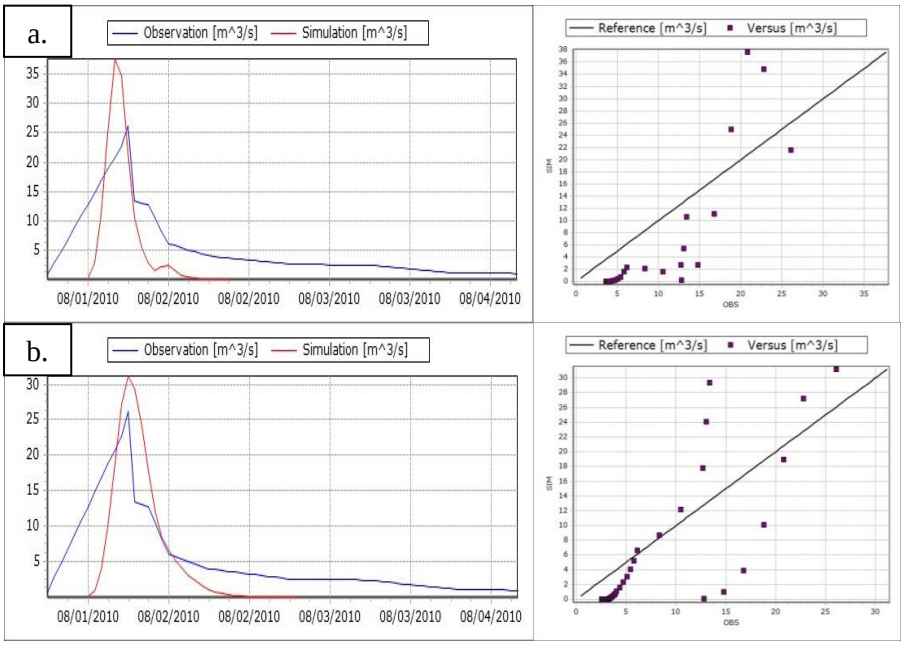

Figure 18. Comparison between the measured and estimated runoff hydrographs at s.h. Covasna based on: a. CN-TAB and computed T_{lag}; b. CN-AF_O and defined T_{lag}.

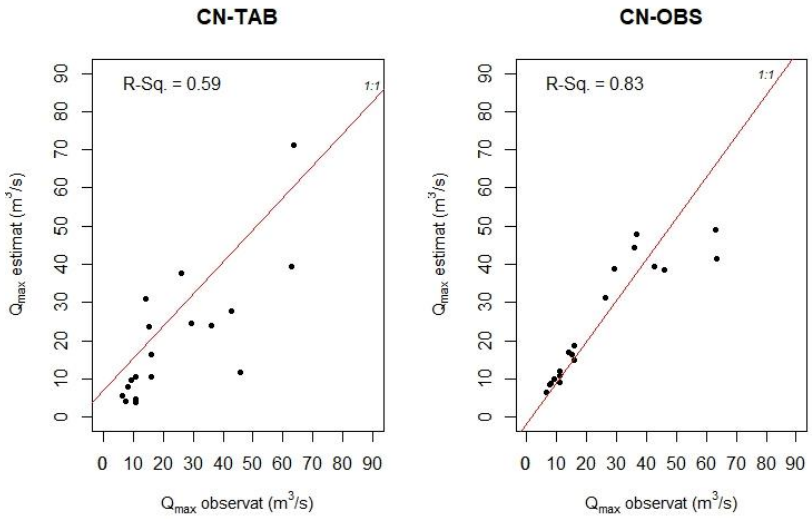

Figure 19. Comparison between estimated and observed peak flows for CN-TAB şi CN-OBS.

6.5. Applications of the semi-distributed model in HEC-HMS and results. A case study on Covasna and Ozunca watersheds

The application of the semi-distributed model for the **Covasna** River basin involved a comparative analysis of two different transform methods: the SCS and the Snyder hydrograph method. Simulated peak flows occured faster, about 3 hours earlier in the case of SCS-UH transform method, compared to the Snyder one (Table 21).

According to the measured data, the river reached its highest level corresponding to a peak flow of 16 m^3/s (410.3 $l/s/km^2$) at 12 a.m. on June 11, 2011. It was observed that the simulated peak flow using the SCS method was much higher than the observed one (a difference of 4.9 m^3/s) and also higher than the one estimated through the Snyder method, with a time difference of about 3 hours, whereas the results obtained with the SCS method (classical procedure) using the lumped- parameter model, revealed a difference in the timing of peak flows of only one hour. The peak flow obtained for the Snyder transform method was slightly lower, by only 1.3%, compared to the observed one, with a minor difference of about 10 min. in the timing of peak flows (Figure 20).

Table 21. Simulated peak discharges for both transform methods in the case of Covasna watershed (Strapazan & Petruț, 2017)

Hydrologic element (River/Subbasin/ Junction)	**SCS**		**Time of peak**	**Snyder**		**Time of peak**
	Q_{max} (m^3/s)	**q ($l/s/km^2$)**		**Q_{max} (m^3/s)**	**q ($l/s/km^2$)**	
Junction-1	6.7	692.9	10.06.2011, 21:51	5.0	517.1	11.06.2011, 00:33
Chetag	4.4	483.5	10.06.2011, 21:55	3.3	362.6	11.06.2011, 00:34
Tistopic	2.3	454.5	10.06.2011, 21:44	1.7	336.0	11.06.2011, 00:32
Junction-3	4.8	556.8	10.06.2011, 20:48	3.4	394.4	11.06.2011, 00:09
Junction-2	2.7	600.0	10.06.2011, 20:47	1.9	422.2	11.06.2011, 00:08
Subbasin-2	1.5	517.2	10.06.2011, 21:10	1.1	379.3	11.06.2011, 00:19
Junction-5	15.4	485.5	10.06.2011, 21:08	11.8	372.0	11.06.2011, 00:16
Junction -4	12.2	472.5	10.06.2011, 21:15	9.5	367.9	11.06.2011, 00:18
Junction -3	2.2	488.9	10.06.2011, 21:11	1.6	355.6	11.06.2011, 00:20
COVASNA Post (Sink-1)	20.9	535.9	10.06.2011, 20:57	15.8	405.1	11.06.2011, 00:11
Junction-7	20.1	523.4	10.06.2011, 21:01	15.2	395.8	11.06.2011, 00:13

For the **Ozunca** study case, the model was applied to the major event that occurred on June 28-29, 2016. This time, the results are presented only for the SCS transform method, given its good performance from the begining. The inflows were simulated, as in the previous case, at each junction within the catchment area (Table 22). A difference of only 2 minutes was observed in the timing of the peak flows, which is much smaller than the one obtained through the lumped-parameter model, with an error of only 9%. In this case, the peak flows were slightly underestimated compared to the results generated by the lumped-parameter model.

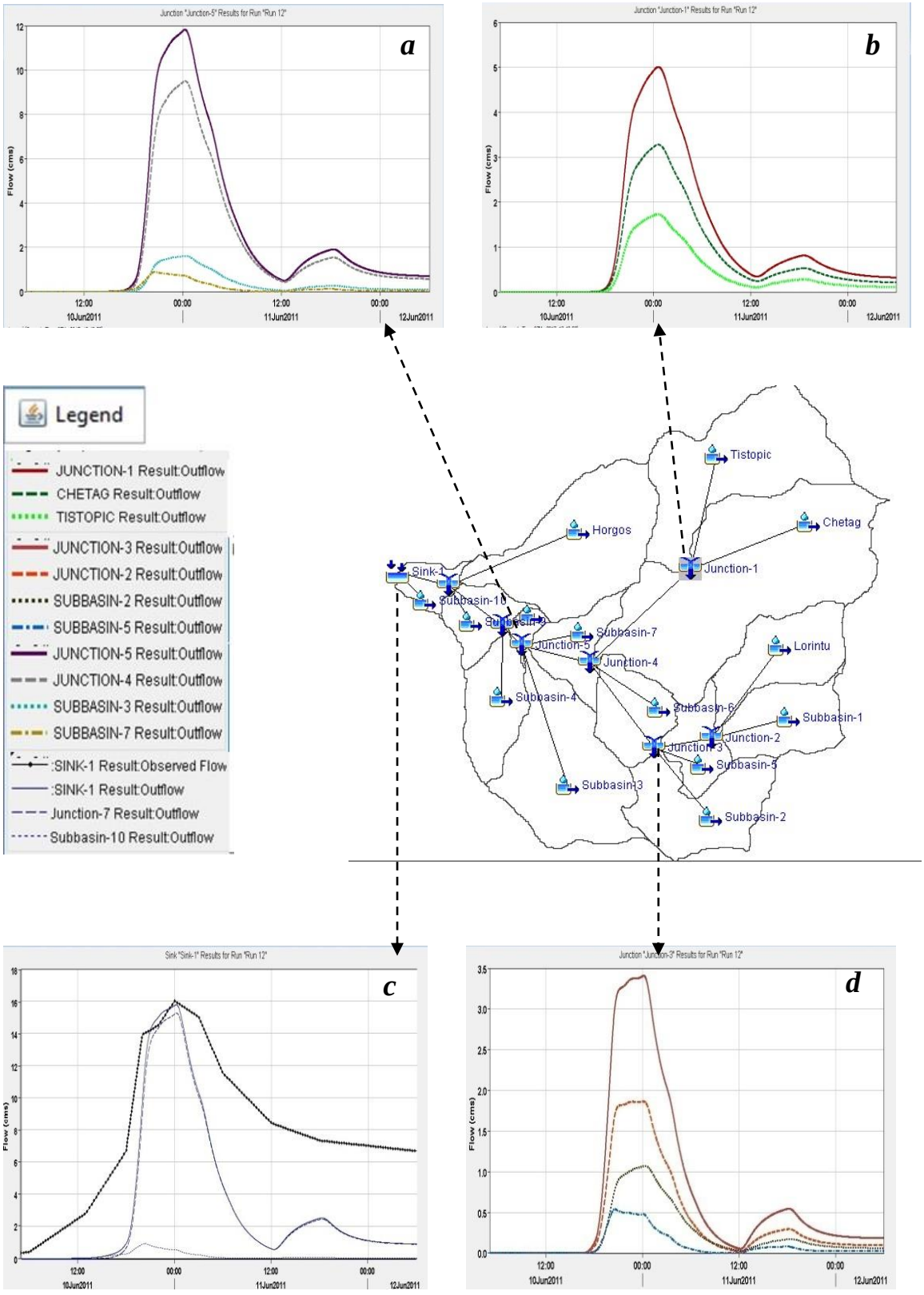

Figure 20. The semi-distributed structure of the HEC-HMS model for the Snyder method-the runoff hydrographs-Covasna. Note:a- at Junction 5; b- at Junction 1;; c-at the gauging station; d-at Junction 3 (Strapazan & Petruț, 2017)

Table 22. Simulated peak flows based on the SCS method for Ozunca watershed

Hydrologic element (River/Subbasin/ Junction)	SCS		Time of peak
	Q_{max} (m^3/s)	q ($l/s/km^2$)	
Junction-207	9.4	1836.6	28.06.2016, 22:04
W730	2.1	1926.6	28.06.2016, 21:50
W810	7.4	1827.2	28.06.2016, 22:07
Junction-216	15.7	580.6	28.06.2016, 22:09
W690	1.2	568.7	28.06.2016, 21:54
W700	1.5	724.6	28.06.2016, 21:56
Junction-210	5.3	1373.1	28.06.2016, 21:54
W640	4.2	1463.4	28.06.2016, 21:55
W720	1.1	1111.1	28.06.2016, 21:51
BĂȚANII MARI Post (Sink-1)	58.0	876.1	28.06.2016, 22:28

6.6. Applications of the Cluj Model and results.

The events used for the distributed-parameter model application are the ones for which gauge-corrected radar-based estimates were used, taking into account the distributed structure of the model. The GIS-based CN calibration algorithm was employed to obtain an average representative value at the basin level as close as possible to the one associated with the lumped-parameter model's optimal results.

For the **Teliu** study case, the CNs were calibrated by up to 39% in order to match the corresponding CN-AM value (85). This computed time of concentration is 1761 min., corresponding to K=0.02. The values of R^2, d, and NSE were much lower, even negative in this case (Table 23), as opposed not only to the previously obtained values for CN-AM but also to those generated through the classical procedure, leading to the conclusion that for the 2018 event, the lumped-parameter model seems to be more suitable.

Table 23. Results of the simulation based on the SCS method and the Cluj model for the Teliu watershed

Event	Observed peak flow		Simulated peak flow		Calibrated parameters		Statistical indicators				
	m^3/s	Time of peak	m^3/s	Time of peak	CN; S	+39% CN_{med} = 84.8	*PEP (%)*	*RMSE*	R^2	*NSE*	*d*
29.06-01.07. 2018	63.0	30.06 - 15:00-16:00	46.2	30.06 – 09:35	K (velocity)	0.02	27	16.38	0.25	<0	0.62

**Where CN_{med} = average CN value obtained through calibration*

For the **Timiș** study case, the CN values needed an adjustment of up to 89% in order to determine an average value as close as possible to the corresponding CN-MD (76.5), considering that the rainfall amount recorded at m.s. Predeal prior to the onset of the event would have classified the condition as AMC I (Table 24). However, the resulting mean value

was far lower (70.0), rather comparable to that associated with CN-AF_O. The computed time of concentration is 586 min. corresponding to *K*=0.3. The error in estimating peak flows was only 0.05, much smaller than that resulting from the application of the lumped-parameter model, both for CN-MD and CN-AF_O. Nevertheless, higher *RMSE* and lower *NSE* values indicated peak flows overestimation, such that the lumped model provided better results.

Table 24. Results of the simulation based on the SCS method and the Cluj model for the Timiș watershed

Event	Observed peak flow		Simulated peak flow		Calibrated parameters		Statistical indicators				
	m^3/s	Time of peak	m^3/s	Time of peak	CN; S	+89% CN_{med} = 70.0	*PEP (%)*	*RMSE*	R^2	*NSE*	*d*
01-02.08. 2010	45.8	01.08 - 20:30	48.0	01.08 – 22:05	K (velocity)	0.3	5	9.99	0.77	0.001	0.85

**Where CN_{med} = average CN value obtained through calibration*

Regarding the **Ozunca** River basin, the CN values were calibrated by up to 20%, resulting in an average CN of 80.1, very close to that of CN-AF_O (79.6). Following the calibration, a runoff depth ranging from 0.55 to 57.6 mm was determined, along with a time of concentration of about 1173 min. corresponding to *K* = 0.1 (Figure 21).

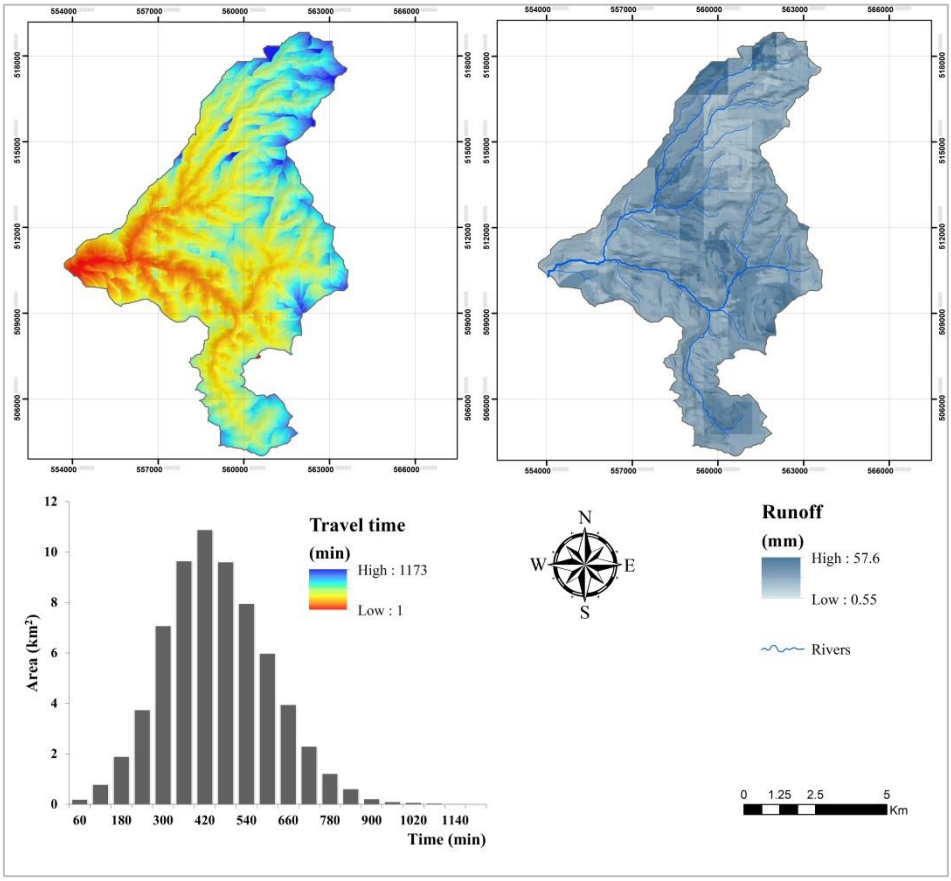

Figure 21. The travel time map with the time-area diagram (left) and the surface runoff depth (right) for Ozunca watershed

There error in estimating peak flow was about 3%, much smaller than that determined for CN-AF_O by the lumped-parameter model, and the R^2 and *d* values were relatively similar. However, results revealed much lower *NSE* values (50%) and somewhat higher *RMSE* for this case (Table 25). The comparison between the estimated and observed hydrographs can be observed in Figure 22.

Table 25. Results of the simulation based on the SCS method and the Cluj model for the Ozunca watershed

Event	Observed peak flow		Simulated peak flow		Calibrated parameters		Statistical indicators				
	m^3/s	Time of peak	m^3/s	Time of peak	CN; S	+20% CN_{med} = 80.1	*PEP (%)*	*RMSE*	R^2	*NSE*	*d*
07-08.05. 2005	36.0	07.05 - 17:30	37.2	07.05 – 17:11	K (velocity)	0.1	3	6.55	0.84	0.33	0.89

Where CN_{med} = average CN value obtained through calibration

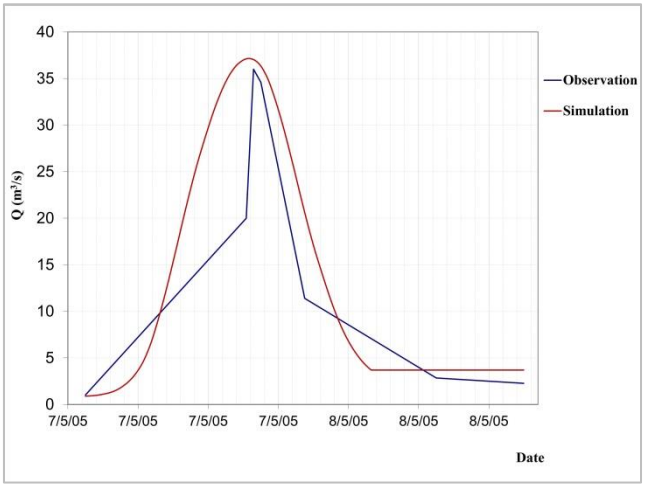

Figure 22. Comparison between observed and estimated runoff hydrographs for h.s. Bățanii Mari (07-08.05.2005 event) based on the SCS method and the Cluj Model

For the **Covasna** study case, the CN values were adjusted by up to 35% in roder to match the one corresponding to CN-AF_O (82). A time of concentration of about 1068 min was determined, corresponding to K = 0.05. A general tendency for peak flow overestimation was noted, but with slightly lower *PEP* and *RMSE* and higher R^2 and *d* values, compared to those obtained through the lumped-parameter model (Table 26). However, the *NSE* value was much lower.

Table 26. Results of the simulation based on the SCS method and the Cluj model for the Covasna watershed

Event	Observed peak flow		Simulated peak flow		Calibrated parameters		Statistical indicators				
	m^3/s	**Time of peak**	**m^3/s**	**Time of peak**	**CN; S**	**+35% CN_{med} = 82**	***PEP (%)***	***RMSE***	***R^2***	***NSE***	***d***
01-02.08 2010	26.1	01.08 - 18:00	30.4	01.08 – 15:52	K (velocity)	0.05	17	4.61	0.89	0.47	0.92

Where CN_{med} = average CN value obtained through calibration

CONCLUSIONS

This research has provided an alternative approach to using the NRCS-CN method for surface runoff and flood events estimation in small-sized mountainous watersheds. Although the rainfall-runoff data-based methods employed for CN estimation revealed some sort of similarity among the obtained results, they differ significantly from those determined through the traditional procedure of using the predefined tables. This demonstrates that certain assumptions made about typical hydrological conditions, do not always apply to different climatic or geographical features, other than those associated with the region or area for which they were created.

Although the alternative CN approach, in this case, provided reliable results it is not certain that these particular results can be extrapolated to a generalized larger scale. Considering that the study watersheds drain a quasi-homogeneous mountainous area, the information may be transferred to similar neighboring ungauged basins. However, further studies should be undertaken in order to identify such comparable drainage areas.

However, generalization and extrapolation to a regional, larger scale involves uncertainties, given the significantly different natural conditions and terrain characteristics, since the rivers flow towards the Brașov Depression. Thus, future work regarding surface runoff modeling from small, forested basins is needed in order to verify or validate the NEH630 tables based on field measurements and observations, especially from the hydrometric stations of the Romanian Waters National Administration. The continuation of this research direction could even involve further redefinition of these values if significant differences are to be identified.

The present findings have shown the lower accuracy provided by the traditional procedure of deriving the CN values from the NEH-630 lookup tables employed for runoff depth estimation in the study area both for $\lambda = 0.2$ and $\lambda = 0.05$. However, when the flood

events simulations were conducted with the rainfall-runoff-based CN values optimal or at least reasonable results were achieved.

Furthermore, comparable results were obtained through the distributed-parameter model, although based on considerably adjusted CN values, confirming yet again the validity of the presented methodology, and also the utility of the implemented GIS-based flow velocity calculation algorithm. The algorithm basically offers an alternative to pluvial floods estimation automating the process required for the distributed-parameter model application. However, further studies are recommended in order to validate its utility based on multiple data series. Additionally, more accurate results could be obtained from high-resolution data using the distributed model. Therefore, this study can serve as a basis for future research regarding the redefinition of CN parameter values which can be used for the calibration and subsequent validation of both lumped and distributed models for runoff and flood events simulation.

SELECTIVE BIBLIOGRAPHY

1. Abbott, M. B & Refsgaard, J. C. (1996). *Distributed Hydrological Modelling*, Kluwer Academic Publishers, Dordrecht, Olanda.
2. Ajmal, M., Kim, T. W. & Ahn, J. H. (2016). Stability assessment of the curve number methodology used to estimate excess rainfall in forest-dominated watersheds. *Arab J Geosci 9*, 402. https://doi.org/10.1007/s12517-016-2421-y
3. Al-Smadi, M. (1998). *Incorporating Spatial and Temporal Variation of Watershed Response in a GIS-based hydrologic model*. MS Thesis, Faculty of the Virginia Polytechnic Institute and State University, Blacksburg, disponibil online la: https://vtechworks.lib.vt.edu/handle/10919/36216, accesat în 02.08.2018.
4. Bălan, I., Crenganiș, L. & Corduneanu, F. (2016). Flood analysis using Mike 11 by DHI and ArcGIS. Case study – the flood in the upper catchment of river Geru, Galaţi county, Romania. RevCAD Journal of Geodesy and Cadastre, 20, 27-38.
5. Beven, K. (2012). *Rainfall-Runoff Modelling. The Primer.* Second Edition, John Wiley & Sons, Ltd, Chichester, West Sussex, UK.
6. Calero Mosquera, D., Hoyos Villada, F. & Torres Prieto, E. (2021). Runoff Curve Number (CN model) Evaluation Under Tropical Conditions. *Earth Sciences Research Journal, 25(4),* 397-404.

7. Cao, H., Vervoort, R. W., & Dabney, S. M. (2011). Variation in curve numbers derived from plot runoff data for New South Wales (Australia). *Hydrological Processes*, *25*(24), 3774–3789. https://doi.org/10.1002/hyp.8102

8. Chendeș, V. (2007). *Scurgerea lichidă și solidă în Subcarpații de la Curbură*. Teza de doctorat. Institutul de Geografie. Academia Română.

9. Chendeș, V. (2011). *Resursele de apă din Subcarpații de la Curbură. Evaluări Geospațiale*. Editura Academiei Române, București, România.

10. Chow, V.T., Maidment, D. R. & Mays, L.W. (1988). *Applied hydrology*. McGraw-Hill Book Company, New York, NY.

11. Cole, B., Smith, G., De La Barreda-Bautista, B., Hamer, A., Payne, M. J., Codd, T., Johnson, S. J., Chan, L. Y., & Balzter, H. (2022). Dynamic Landscapes in the UK Driven by Pressures from Energy Production and Forestry—Results of the CORINE Land Cover Map 2018. *Land*, *11*(2), 192. https://doi.org/10.3390/land11020192

12. Corbuș C. (2010). *Programul CAVIS pentru determinarea caracteristicilor undelor de viitură singulare*. In: Conferinţa Ştiinţifică Jubiliară a Institutului Naţional de Hidrologie şi Gospodărirea Apelor, ”Hidrologia şi gospodărirea apelor - Provocări 2025 pentru dezvoltarea durabilă a resurselor de apă”, București, 116-123.

13. Costache, R. (2014) Using GIS techniques for assessing lag time and concentration time in small river basins. Case study: Pecineaga river basin, Romania. *Geographia Technica*, *9* (1),31-38.

14. Crăciun, A. I. (2011). *Estimarea indirectă, cu ajutorul GIS, a umezelii solului în scopul modelării viiturilor pluviale. Aplicatții în Munții Apuseni* (Teză de doctorat). Universitatea Babeș-Bolyai, Cluj-Napoca, România.

15. Crăciun, A. I., Haidu, I., Magyari-Sáska, Zs. & Imbroane, A. I. (2009). Estimation of runoff coefficient according to soil moisture using GIS techniques. *Geographia Technica*, *4*(2), 1-10.

16. D’Asaro F, Grillone G, Hawkins RH**,** (2014). Curve number: empirical evaluation and comparison with curve number handbook tables in Sicily. *J Hydrol Eng. 19*(12) :04014035. https://doi.org/10.1061/(asce)he.1943-5584.0000997

17. DHI (2017). Danish Hydraulic Institute. *MIKE 1D.DHI Simulation Engine for 1D river and urban modeling. Reference Manual*. DHI, Horsholm, Denmark.

18. Diaz-Ramirez J. N., McAnally W. H. & Martin, J. L. (2011). Analysis of hydrological processes applying the HSPF model in selected watersheds in Alabama, Mississippi, and

Puerto Rico. *Applied Engineering in Agriculture, 27*(6):937–954. https://doi.org/10.13031/2013.40627

19. Domnița, M. (2012). *Runoff modeling using GIS. Application in torrential basins in the Apuseni Mountains* (Ph.D Thesis), Universitatea Babeș-Bolyai, Cluj-Napoca, România.

20. Drobot, R. (2007). *Metodologia de dereminare a bazinelor hidrografice torențiale în care se află așezări umane expuse pericolului viiturilor rapide.* Departamentul de Cercetare și Proiectare în Construcții - Universitatea Tehnică de Construcții București, România.

21. Du, J., Xie, H., Hu, Y., Xu, Y., Xu & C.Y. (2009). Development and testing of a new storm runoff routing approach based on time variant spatially distributed travel time method. *J. Hydrol. 369*(1–2), 44–54. https://doi.org/10.1016/j.jhydrol.2009.02.033.

22. Elzhov, T. V., Mullen, K. M., Spiess, A.-N. & Bolker, B. (2016). minpack.lm: R interface to the Levenberg-Marquardt nonlinear least-squares algorithm found in MINPACK, plus support for bounds. R package version 1.2-1. Disponibil online la: https://CRAN.R-project.org/package=minpack.lm, accesat în 03.08.2022.

23. Gyori, M. M. & Haidu, I. (2011). Unit Hydrograph generation for ungauged subwatersheds. Case study: The Monoroștia River, Arad County, Romania. *Geographia Technica*, *6*(2), 23-29.

24. Gyori, M. M. (2013). *Predicția viiturilor rapide în condiții de date limitate.Aplicații la râurile mici din munții Zărandului și Săvârnișului* (Teză de doctorat). Universitatea Babeș-Bolyai, Cluj-Napoca, România.

25. Gyori, M. M., Haidu, I. & Humbert, J. (2016). Deriving the floodplain in rural areas for high exceedance Probability Having Limited Data Source. *Environ Eng Manag J, 15* (8), 1879-1887. https://doi.org/10.30638/eemj.2016.201

26. Gyori, M. M., Humbert, J. & Haidu, I. (2013). Deriving flash floods in the case of simulated precipitations. *Geographia Napocensis, 7* (2), 11-18.

27. Haidu, I. & Ivan, K. (2016). Évolution du ruissellement et du volume d'eau ruisselé en surface urbaine. Étude de cas : Bordeaux 1984- 2014, France. *La Houille Blanche,* 5, 1-6.

28. Haidu, I. & **Strapazan**, C. (2019). Flash flood prediction in small to medium-sized watersheds. Case study: Bistra river (Apuseni Mountains, Romania). *Carpathian J. Earth Environ. Sci. 14*(2), 439–448. https://doi.10.26471/cjees/2019/014/093

29. Hänsel, S., Hoy, A., Brendel, C., Maugeri, M. (2022). Record summers in Europe: Variations in drought and heavy precipitation during 1901–2018. *Int. J. Climatol., 42*, 6235–6257. https://doi.org/10.1002/joc.7587

30. Hawkins, R. H. (1993). Asymptotic determination of runoff curve numbers from data. *J Irrigat Drain Eng*., *119*(2), 334–345. https://doi.org/10.1061/(asce)0733-9437(1993)119:2(334

31. Hawkins, R. H., Hjelmfelt, A. T., & Zevenbergen, A. W. (1985). Runoff Probability, Storm Depth, and Curve Numbers. *Journal of Irrigation and Drainage Engineering*, *111*(4), 330–340. https://doi.org/10.1061/(asce)0733-9437(1985)111:4(330

32. Hawkins, R. H., Theurer, F. D. & Rezaeianzadeh, M. (2019). Understanding the basis of the curve number method for watershed models and TMDLs. *J. Hydrol. Eng.*, 24, 06019003. https://doi.org.10.1061/(ASCE)HE.1943-5584.0001755.

33. Hawkins, R. H., Ward, T.J., Woodward, D.E. & Van Mullem J.A. (2009). *Curve number hydrology-state of practice.* The ASCE/EWRI publication, U.S. ISBN. 978–0-7844-7257-6

34. Hjelmfelt, A. T. (1991). Investigation of curve number procedure. *J. Hydr. Engrg.*, ASCE, *117*(6), 725-737.

35. Ibrahim, S., Brasi, B., Yu, Q. & Siddig, M. S. (2022). Curve number estimation using rainfall and runoff data from five catchments in Sudan. *Open Geosciences*, *14*(1), 294 - 303. https://doi.org/10.1515/geo-2022-0356

36. Im, S., Lee, J., Kuraji, K., Lai, Y. J., Tuankrua, V., Tanaka, N., Gomyo, M., Inoue, H. & Tseng, C.W. (2020). Soil Conservation Service curve number determination for forest cover using rainfall and runoff data in experimental forests. *Journal of Forest Research*, *25*(4): 204-213. https://doi.org/10.1080/13416979.2020.1785072

37. Institutul de Meteorologie şi Hidrologie (1971). *Râurile României. Monografie hidrologică*, București.

38. Ivănescu, V., Mocanu, P., & Sandu, M.A. (2014). Application of a hydrodynamic MIKE 11 Model for Argesel river. In: 14th International Multidisciplinary Scientific Geoconference. GeoConference on Water Resources.Forest, Marine and Ocean Ecosystem. Conference Proceedings, Albena, Bulgaria, 65-72.

39. Kaffai-Vodă, A. I. (2022). *Scurgerea maximă în bazinele hidrografice nemonitorizate de mici dimensiuni. Studii de caz în bazinul hidrografic Mureș* (Teză de doctorat). Universitatea Babeș-Bolyai, Cluj-Napoca, România.

40. Khaddor, I. & Alaoui, A. H. (2014). Production of a Curve Number map for Hydrological simulation - Case study: Kalaya Watershed located in Northern Morocco. *International Journal of Innovation and Applied Studies*, *9*(4), 1691-1699.

41. Kocsis, I., Haidu, I., Maier, N. (2020) Application of a Hydrological MIKE HYDRO River – UHM Model for Valea Rea River (Romania). Case Study, Flash Flood Event Occurred on August 1st, 2019. 2020 ”Air and Water – Components of the Environment” Conference Proceedings, Cluj-Napoca, Romania, 257-272, https://doi.org/10.24193/AWC2020_24.

42. Kowalik, T. & Walega, A. (2015). Estimation of CN parameter for small agricultura watersheds using asymptotic functions. *Water*, *7*(3), 939-955. https://doi.org/10.3390/w7030939

43. Kraemer, C. & Panda, S. S. (2009). Automating ArcHydro for watershed delineation,In: The University of Georgia, Water Resources Faculty (ed.). *Proceedings of the 2009 Georgia Water Resources Conference*. Athens, Georgia U.S.A, Warnell School of Forestry and Natural Resources, The University of Georgia, 428-433.

44. Man, T. & Alexe, M. (2006). Modelare hidrologică în GIS. Implementarea Modelului SCS-CN pentru evaluarea scurgerii. *Geographia Technica*, 1, 121-126.

45. Mishra, S. K. & Singh, V. P. (2003). *Soil Conservation Service Curve Number (SCS-CN) Methodology*. Volume 42. Water Science and Technology Library, Springer, Netherlands, Dordrecht.

46. Mishra, S. K., Jain, M. K., Babu, P. S., Venugopal, K. & Kaliappan, S. (2008). *Comparison of AMC-dependent CN-conversion formulae*. Water Resources Management 22(10):1409–1420. https://doi.org/10.1007/s11269-007-9233-5

47. Moriasi, D. N., Arnold, J. G., Van Liew, M. W., Bingner, R. L., Harmel, R. D. & Veith, T. L. (2007). Model evaluation guidelines for systematic quantification of accuracy in watershed simulations. *Transactions of the of the American Society of Agricultural and Biological Engineers*, 50(3), 885-900. https://doi.org/10.13031/2013.23153.

48. Mouratidis, A., & Ampatzidis, D. (2019). European Digital Elevation Model Validation against Extensive Global Navigation Satellite Systems Data and Comparison with SRTM DEM and ASTER GDEM in Central Macedonia (Greece). *ISPRS International Journal of Geo-information*, *8*(3), 108. https://doi.org/10.3390/ijgi8030108

49. Mustățea, A. (2005). *Viituri excepționale pe teritoriul României. Geneză și efecte*. Editura București.

50. Musy, A. & Higy, C. (1998). *Hydrologie appliquée*. Editions H*G*A, Bucureşti. ISBN: 973-98530-8-0;

51. NRCS (2004). *Chapter 9 Hydrologic Soil-Cover complexes*. In Part 630 Hydrology National Engineering Handbook. Natural Resources Conservation Service, U.S.D.A.: Washington, DC.

52. Olaya, V. (2004a). *A gentle introduction to SAGA GIS*. Edition 1.1. The SAGA User Group, Göettingen University, Germany (disponibil la: https://sourceforge.net/projects/saga-gis/files/SAGA%20-%20Documentation/SAGA%20Documents/, accesat în 05.01.2018)

53. Olaya, V. (2004b). *Hidrología Computacional y Modelos Digitales del Terreno-Teoría, Práctica y Filosofía de una Nueva Forma de Análisis Hidrológico*. Editora: Madrid, Spain.

54. Ponce, V. M., & Hawkins, R. H. (1996). Runoff curve number: Has it reached maturity? *J. Hydrol. Eng.*, 1(1), 11–19. https://doi.org/10.1061/(asce)1084-0699(1996)1:1(11

55. Ritter, A. & Muñoz-Carpena, R. (2013). Performance evaluation of hydrological models: Statistical significance for reducing subjectivity in goodness-of-fit assessments. *J. Hydrol.*, 480, 33–45.

56. SCS (1964). *Soil Conservation Service. National Engineering Handbook, Section 4: Hydrology*; U.S. Soil Conservation Service: Washington, DC, USA, 1964.

57. Steiner, M., Smith, J. A., Burges, S. J., Alonso, C., & Darden, R. W. (1999). Effect of bias adjustment and rain gauge data quality control on radar rainfall estimation. *Water Resources Research*, *35*(8), 2487–2503. https://doi.org/10.1029/1999wr900142

58. **Strapazan**, C. & Petruț, M. (2017). Application of Arc Hydro and HEC-HMS model techniques for runoff simulation in the headwater areas of Covasna Watershed (Romania). *Geographia Technica*, *12*(1), 95-107. https://doi.10.21163/GT_2017.121.10.

59. **Strapazan**, C., Haidu, I. & Kocsis, I. (2019). Assessing Land Use/Land Cover Change and its Impact on Surface Runoff in the Southern Part of the Țibleș and Rodnei Mountains. In: Air and Water – Components of the Environment Conference Proceedings, Cluj-Napoca, Romania, 225-236. https://doi.10.24193/AWC2019_23.

60. **Strapazan**, C., Haidu, I., & Irimuș, I. A. (2021). A comparative assessment of different loss methods available in Mike Hydro River – UHM. *Carpathian Journal of Earth and Environmental Sciences*, *16*(1), 261-273. https://doi.10.26471/cjees/2021/016/172

61. **Strapazan**, C., Irimuș, I.-A., Șerban, G., Man, T.C. & Sassebes, L. (2023a). Determination of Runoff Curve Numbers for the Growing Season Based on the Rainfall–Runoff Relationship from Small Watersheds in the Middle Mountainous Area of Romania. *Water*, 15, 1452. https://doi.org/10.3390/ w15081452

62. **Strapazan**, C., Kocsis, I., Irimuș, I.-A. & Balint-Balint, L. (2023b). An evaluation of LIDAR, EU-DEM And SRTM-derived terrain parameters for hydrologic applications in Țibleș and Rodnei Mountains. *Riscuri și catastrofe*, *32*(1), 20. https://doi.org/10.24193/RCJ2023_1

63. Talchabhadel, R., Shakya, N.M., Dahal, V. & Eslamian, S. (2015). Rainfall Runoff Modelling for Flood Forecasting (A Case Study on West Rapti Watershed), Journal of Flood Engineering, 6, 1, 53-61

64. Tedela, N. H., McCutcheon, S. C., Rasmussen, T. C., Hawkins, R. H., Swank, W. T., Campbell, J. L., Adams, M. B., Jackson, C. R. & Tollner, E.W. (2012). Runoff curve numbers for 10 small forested watersheds in the mountains of the eastern United States. *J. Hydrol. Eng.*, *17*, 1188–1198. https://doi.org/10.1061/(asce)he.1943-5584.0000436

65. Tsanakas, K., Gaki-Papanastassiou, K., Kalogeropoulos, K., Chalkias, C., Katsafados, P., & Karymbalis, E. (2016). Investigation of flash flood natural causes of Xirolaki Torrent, Northern Greece based on GIS modeling and geomorphological analysis. *Natural Hazards*, *84*(2), 1015–1033. https://doi.org/10.1007/s11069-016-2471-1.

66. USACE (1998). *HEC-1.Flood Hydrograph Package. User's manual.* Hydrologic Engineering Center, Davis, CA U.S.A

67. USACE (2000). *Hydrologic Modeling System HEC-HMS, Technical Reference Manual*. Hydrologic Engineering Center, Davis, CA U.S.A,.

68. USDA-NRCS, (1986). *Urban Hydrology for Small Watersheds*. 210-VI-TR-55, Second Ed., U. S. Dept. of Agriculture, Washington D. C.:

69. Woodward, D. E., Hawkins, R. H., Jiang, R., Hjelmfelt Junior, A. T., Van Mullem, J. A. & Quan, D. Q (2003). Runoff curve number method: examination of the initial abstraction ratio. In: 2003 World Water And Environmental Resources Congress, Philadelphia. Proceedings Reston: ASCE,. 1-10. https://doi.org/10.1061/40685(2003)308

70. Zaharia, L., Bui, D. T., Prăvălie, R., & Ioana-Toroimac, G. (2017). Mapping flood and flooding potential indices: a methodological approach to identifying areas susceptible to flood and flooding risk. Case study: the Prahova catchment (Romania). *Frontiers of Earth Science*, *11*(2), 229–247. https://doi.org/10.1007/s11707-017-0636-1

71. Zambrano-Bigiarini, M. (2020). *Package hydroGOF: Goodness-of-fit functions for comparison of simulated and observed hydrological time series*. Disponibil online la: https://cran.r-project.org/web/packages/hydroGOF/ hydroGOF.pdf, R package version 0.4- 0, accesat în 15.06.2022.

72. Zhang, X., & Srinivasan, R. (2010). GIS-based spatial precipitation estimation using next generation radar and raingauge data. *Environmental Modelling and Software*, *25*(12), 1781–1788. https://doi.org/10.1016/j.envsoft.2010.05.012

73. *** EEA (2017). *European Environment Agency, Copernicus Land Monitoring Service*. *CLC 2006.* Disponibil online la: https://land.copernicus.eu/pan-european/corine-land-cover/clc-2006, accesat în 06.01.2017.

74. *** EEA (2018). *European Environment Agency, Copernicus Land Monitoring Service*. *CLC 2012.* Disponibil online la: https://land.copernicus.eu/pan-european/corine-land-cover/clc-2012, accesat în 06.12.2018.

75. *** EEA (2020). *European Environment Agency, Copernicus Land Monitoring Service*. *CLC 2018*. Disponibil online la: https://land.copernicus.eu/pan-european/corine-land-cover/clc2018, accesat în 04.01.2020

76. *** https://geoportal.igr.ro/viewgeol200k, accesat în 11.09.2022

77. *** METEOMANZ (2017). *SYNOP/BUFR observations. Data by hours.* Disponibil online la: http://www.meteomanz.com/, accesat în 05.06.2017

78. *** R Core Team (2022). *R: A language and environment for statistical computing. R Foundation for Statistical Computing*, Vienna, Austria. Disponibil online la: https://www.R-project.org/, accesat în 10.07.2022

79. *** RP5 (2017). *Reliable prognosis*. Disponibil online la: https://rp5.ru/ , accesat în 04.06.2017

80. *** RStudio Team (2022), *RStudio: Integrated Development Environment for R.* Rstudio. PBC, Boston, MA. Disponibil online la: http://www.rstudio.com/, accesat în 10.07.2022

81. *** The MathWorks Inc. (2023). MATLAB version: 9.14.0 (R2023a) Update 2, disponibil la: https://matlab.mathworks.com/, accesat în 26.04.2023.